

# Few EURONEAR NEA mini-surveys observed with the INT, KASI and T80S telescopes during the ParaSOL synthetic tracking project <sup>\*,\*\*</sup>

O. Vaduvescu<sup>a,b,c</sup>, M. Stanescu<sup>d,e</sup>, M. Popescu<sup>d,a</sup>, M. Predatu<sup>a</sup>, L. Curelaru<sup>d</sup>,  
D. Bertesteanu<sup>d,e</sup>, C. Boldea<sup>a</sup>, F. Ursache<sup>f</sup>, C. Fotin<sup>g</sup>, C. de la Fuente Marcos<sup>h</sup>,  
R. de la Fuente Marcos<sup>h</sup>, E. Unda-Sanzana<sup>i</sup>, F. Barwell<sup>b,j</sup>, K. Jhass<sup>b</sup>, S. Shenoy<sup>b,k</sup>,  
A. Santos-Garcia<sup>b,l</sup>, J. Bishop<sup>b</sup>, J. Munday<sup>m,b</sup>, J. de Leon<sup>c</sup>, C.-U. Lee<sup>n</sup>, D.-J. Kim<sup>n</sup> and  
C. Mendes de Oliveira<sup>o</sup>

<sup>a</sup>University of Craiova, Str. A. I. Cuza 13, 200585, Craiova, Romania

<sup>b</sup>Isaac Newton Group (ING), Apt. de correos 321, Santa Cruz de La Palma, E-38700, Canary Islands, Spain

<sup>c</sup>Instituto de Astrofísica de Canarias (IAC), C/ Vía Lactea s/n, La Laguna, E-38205, Tenerife, Spain

<sup>d</sup>Astronomical Institute of the Romanian Academy, Cutitul de Argint 5, Bucharest, 040557, , Romania

<sup>e</sup>Bucharest Astroclub, B-dul Lascar Catargiu 21, Bucharest, 010663, , Romania

<sup>f</sup>Starhopper Observatory, , Sfântu Gheorghe, , Covasna, Romania

<sup>g</sup>Romanian Society for Meteors and Astronomy (SARM), CP 14 OP 1, Targoviste, 130170, Dambovita, Romania

<sup>h</sup>Universidad Complutense de Madrid, Ciudad Universitaria, Madrid, E-28040, , Spain

<sup>i</sup>Centro de Astronomía (CITEVA), Universidad de Antofagasta, Avda. U. de Antofagasta, 02800, Antofagasta, Chile

<sup>j</sup>Astrophysics Research Cluster, School of Mathematical and Physical Sciences, University of Sheffield, Western Bank, Sheffield, S10 2TN, , UK

<sup>k</sup>Centre for Astrophysics Research, University of Hertfordshire, Hatfield, Hertfordshire, AL10 9AB, , UK

<sup>l</sup>Departament de Física, Universitat Politècnica de Catalunya, c/ Esteve Terrades 5, Castelldefels, 08860, Barcelona, Spain

<sup>m</sup>Department of Physics, University of Warwick, Gibbet Hill Road, Coventry, CV4 7AL, , UK

<sup>n</sup>Korea Astronomy and Space Science Institute, , Daejeon, 34055, , Republic of Korea

<sup>o</sup>Instituto de Astronomia, Geofísica e Ciências Atmosféricas da USP, Cidade Universitária, Sao Paulo, 05508-900, , Brazil

---

## ARTICLE INFO

### Keywords:

Near Earth asteroids  
surveys  
source detection  
synthetic tracking

---

## ABSTRACT

The modern synthetic tracking technique (ST) can make use of small and medium-sized telescopes to detect asteroids fainter than the classic blinking methods, by arbitrary shifting and co-adding more images of the same survey field, if GPU computing resources are available. In the framework of the Romanian ParaSOL project, we developed and tested an innovative ST algorithm capable of detecting in near-real-time very faint near-Earth asteroids (NEAs), which likely became the first ST pipeline developed in Europe. To test our pipeline, we conducted several mini-surveys using three large-field telescopes, namely the ING's INT, the Korean KASI and the Brazilian T80S telescopes. Most images were processed using our *Umbrella Image Processing Pipeline* (IPP) module. The ST search was conducted using our *Synthetic Tracking via Umbrella* (STU) module and the commercial *Tycho Tracker* software, which allowed to compare and complement the findings. The source validation was supported by reducers using our new Webrella platform. Most of the nights were reduced in near-real-time, demonstrating the ability to process, sort, and report large volumes of data. We discovered 5 credited and 4 one-night NEAs, co-discovered other 3 NEAs and recovered 3 poorly known NEAs. We flagged 59 NEA candidates for recovery and orbital classification, discovering, co-discovering and recovering other 18 orbitally related NEAs, additionally improving the orbits of 23,428 known asteroids and reporting 1,374 unknown objects. A comparison between ST and traditional blinking detection using the new EURONEAR tool *MagLim* shows improvements of two magnitudes and a two-fold increase in the number of detections. A preliminary comparison between STU and Tycho shows that STU detects about 70% of Tycho findings, however STU detects rapid objects much faster than Tycho, 7 NEAs with speeds between 2-10"/min being found exclusively by STU. Based on our surveys, we assessed the current NEA discovery rate using 1-2-m class telescopes and ST methods, finding that one NEA candidate can be discovered in every 9-12 square degrees up to magnitude ~ 23.

## 1. Introduction

Early detection and precise orbital characterization of most of the more massive (above 10 meters) near Earth asteroids (NEAs) is crucial mainly for the safety of the mankind. Some major collisions were suggested by mass extinction theories [3] and could be proved by events such as Tunguska [24], Chelyabinsk [10], and more recently by the CNEOS Fireball Database<sup>1</sup>.

### 1.1. NEA Surveys

There are about 1.4 million known asteroids in the Solar System of which more than 36,300 NEAs are known as of 16 October 2024, according to MPC<sup>2</sup>. The rapid progress in the last decades has been made possible mainly thanks to eight major surveys funded by U.S. which have used mostly 1-2 m class telescopes to discover 96% of the current known NEA population members during the past four decades, according to NASA/JPL<sup>3</sup>. In order of number of discoveries, the U.S. based surveys are: Catalina [35] (which discovered 44.5% of total known NEAs), Pan-STARRS [28] (31.7%), LINEAR [51] (7.5%), ATLAS<sup>4</sup> [56] (3.1%, using four 50 cm telescopes), Spacewatch [21, 38] (2.4%), NEAT [42] (1.2%), WISE/NEOWISE [70, 37] (1.0%, 40 cm space-based mission), and LONEOS [11] (counting 0.8%). A few other smaller (mostly private) U.S. based surveys contributed the remaining 3.8%.

A few other surveys based in Europe or elsewhere count together for only 4% NEA discoveries. According to MPEC Watch<sup>5</sup>, the non-U.S. ranking is currently led by GINOP-KHK survey<sup>6</sup> (professional site Piszkesteto Observatory in Hungary, counting 0.63% of total discoveries), MAPS<sup>7</sup> (private site in Chile, 0.56%), MARGO<sup>8</sup> (private site in Ukraine, 0.29%), LSSS<sup>9</sup> (former private site in La Sagra, Spain, 0.21%), Kiso [30, 44] (professional observatory in Japan, 0.15%), Moonbase South Observatory<sup>10</sup> (private site in Namibia, 0.15%), Crni-Vrh<sup>11</sup> (private site in Slovenia, 0.11%), Observatorio Campo dos Amarais<sup>12</sup> (private site in Brazil, 0.07%), then ESA-OGS [34] (ESA's site in Tenerife, Spain, counting 0.06%).

Actually, the non-U.S. contribution has increased during the last years, thanks to the advance in technology which made hardware (GPU video cards, RAM, storage capacity) more accessible for surveys, recovery and follow-up projects using small telescopes (30-60 cm) aperture endowed with large field of views (few square degrees), thanks to the available commercial software *Tycho Tracker*<sup>13</sup> [40].

### 1.2. Blinking and Track and Stack Detection

All major NEA surveys employ blink detection using only 4-5 CCD images of the same field, their detection efficiency being limited mainly by the aperture of the telescope, the observing conditions (seeing, airmass and Moon phase), and proper motion of targets. During the last few years, some of the smaller surveys (such as MAPS, GINOP-KHK, Kiso) started to use CMOS cameras which reduce the overhead to almost zero by acquiring a few dozen images of the same field in order to use synthetic tracking technique able to “freeze” the image of the faster asteroids and enhance the detection limit to above 20 mag.

\* Accepted in New Astronomy, Volume 119, 2025, 102410

\*\* This research project was funded by the Romanian National Authority for Scientific Research (UEFISCDI), being based on observing time awarded on the Isaac Newton Telescope (INT), the Korean Astronomy and Space Science Institute (KASI) and the Brazilian T80S telescopes.

\*Corresponding author

ORCID(s): 0000-0002-5341-2792 ( O. Vaduvescu)

<sup>1</sup><https://cneos.jpl.nasa.gov>

<sup>2</sup><http://www.minorplanetcenter.net>

<sup>3</sup>[https://cneos.jpl.nasa.gov/stats/site\\_all.html](https://cneos.jpl.nasa.gov/stats/site_all.html)

<sup>4</sup><https://atlas.fallingstar.com/>

<sup>5</sup><https://sbnmpc.astro.umd.edu/mpecwatch/obs.html>

<sup>6</sup><http://titan.physx.u-szeged.hu/~sky/jas/>

<sup>7</sup><https://www.spaceobs.com/fr/Blog-de-Alain-Maury/Recherche/Decouvertes-de-MAPS>

<sup>8</sup>[https://en.wikipedia.org/wiki/Gennadiy\\_Borisov](https://en.wikipedia.org/wiki/Gennadiy_Borisov)

<sup>9</sup><http://www.minorplanets.org/OLS/LSSS.html>

<sup>10</sup><https://www.moonbase.pl/>

<sup>11</sup><https://www.observatorij.org/>

<sup>12</sup><https://www.facebook.com/ObservatorioCampoDosAmarais/>

<sup>13</sup><https://www.tycho-tracker.com/>

As part of the EURONEAR project<sup>14</sup> led by Ovidiu Vaduvescu, during the last 18 years we have conducted astrometric projects (NEAs and any other asteroids detected in the observed fields) for the recovery, follow-up and a few survey projects using professional telescopes available in La Palma, Chile and other few sites accessible via usual allocation calls by the PI and other members of the EURONEAR network. During this period, most of manpower came from Romania, thanks to collaborations of the PI mostly with amateur astronomers and students.

Our first astrometric projects took place between 2008-2017 and involved trained remote citizen scientists (students and amateurs) who visually blinked images previously reduced with THELI [46, 45] using *Astrometrica*<sup>15</sup>. The images were taken both from regular observing runs [58, 9, 60, 62, 64, 66] and from imaging archives used for data mining (p)recovery projects lead by the same PI [59, 61, 63, 65, 67]. In addition to blinking detection, one can use the “track and stack” technique to detect known very faint asteroids above the detection limit of a given facility, by co-adding more images upon shifting them based on the expected direction and speed. Using the track and stack option of *Astrometrica*, we recovered hundreds of one-opposition NEAs as faint as  $V \sim 24$  using mostly between 6-12 images taken with the *Isaac Newton Telescope* (INT), a by-product of this work being the first NEAs discovered as part of the EURONEAR project, thanks to the careful visual blinking of the THELI reduced images by a team of few amateur volunteers [66]. Actually, the track and stack technique could be regarded as the progenitor of the modern synthetic tracking technique.

Between 2015-2021 we proposed a PhD project hosted at *Technical University of Cluj-Napoca* which aimed to implement in Python, IRAF [54, 55] and AstrOmatic<sup>16</sup> the first EURONEAR pipeline needed for the automatic reduction of asteroid surveys using the classic blink approach [16, 17].

Related to this project, between 2017-2019 we embarked in the NEARBY project<sup>17</sup>, which aimed to offer an online platform to reduce, detect and validate moving sources via blinking in asteroid surveys. The NEARBY platform consists of a Python cloud-based containerized application for image reduction, moving object detection (linked to a MySQL relational database) and human validation (assisted by GUI, HTML and Bootstrap) accessible through web browsers [49, 50, 6, 26, 68]. We have proved NEARBY first on archival images, then for near-real-time surveys in which we discovered two NEAs with the INT.

Between 2020-2022 we followed NEARBY with the CERES project<sup>18</sup> which improved NEARBY detection using machine learning techniques [5, 7]. These results contributed to another PhD thesis defended at *West University of Timisoara* [57].

Independently of these past projects, between 2015-2019 Malin Stanescu developed the *Umbrella* software suite, a set of Mono/.NET Framework programs written in C#, for image reduction, blink detection and human validation of asteroids [52].

### 1.3. Synthetic Tracking Detection

The “synthetic tracking” technique (ST), also known as “digital tracking” (DT), is a computational method aimed at detecting faint moving sources by combining multiple images of the same region of the sky taken within a short timespan, assuming apparent linear motion of any potential object crossing these images. By aligning and stacking the images along various potential motion paths, the ST method enhances the signal-to-noise ratio (SNR) of moving objects, enabling the detection of objects too faint to be found in single exposures using the traditional blinking method. Thanks to the faster and cheaper GPU capabilities available nowadays, ST represents a great opportunity for small larger field telescopes, including professional (dormant or closed) 1 m class telescopes located in good sites, also continuing to offer a NEO discovery niche for very small private facilities (such as the MAPS survey in Chile).

---

<sup>14</sup><http://www.euronear.org/>

<sup>15</sup><http://www.astrometrica.at>

<sup>16</sup><https://www.astromatic.net/>

<sup>17</sup><https://cgis.utcluj.ro/nearby>

<sup>18</sup><https://cgis.utcluj.ro/ceres>

The DT technique was invented by few U.S.–Canadian researchers, being aimed for deep searches of trans-Neptunians (TNOs) and Kuiper Belt objects (KBOs) which move very slowly through the stars (about 100 times slower than typical NEAs) [15, 23, 22], being also applied in searches of satellites of major planets [29, 31].

The ST terminology was proposed first by a U.S. team [2, 8], but actually the ST and DT terms refer to the same method. These techniques were applied first for very slow targets observed with very large telescopes such as HST, CFHT, Hale, Subaru, Keck [14, 19, 20], Blanco DECam [69], and also in Subaru-HSC archival images [12, 73].

The first automatic DT algorithm able to detect main belt asteroids (MBAs) and later NEAs and space debris was actually published by Japanese researchers of JAXA [71]. They used fast “Field Programmable Gate Arrays” (FPGA), a hardware designed for real-time processing of space observations taken by a small on-board telescope. The JAXA team proved first the use of their FPGA technique for the detection of asteroids on images taken with a small 35-cm ground telescope, discovering a few MBAs up to mag 21 (comparable with blinking images taken by a 1m-class telescopes). Later, this team proved the feasibility of the FPGA technique to discover 11 NEAs by combining dozens of frames captured with 20-cm class ground telescopes [72]. More recently, they proposed a pipeline for automatic streak real-time detection using a multi-GPU system [13], feasible to search flyby NEAs and space debris.

During the last decade, ST was implemented to work with GPU hardware by a JPL team which aimed the detection of very rapid flyby NEAs using very short exposures taken by very fast sCMOS cameras [47, 74] (apparently the first ST publications mentioning the use of GPU), and also [27, 75, 76]. The same team proposed to use ST aboard a NASA/JPL mission SmallSats satellites equipped with 10-20 cm telescopes which could find and track 90% of the NEAs larger than 50 m ( $H \leq 24.2$ ), i.e. brighter than  $V \leq 22.1$  [48].

Between 2022-2024 we embarked in the Romanian ParaSOL project<sup>19</sup>, aiming to create a tracking-pipeline framework based on elements of the Umbrella software suite for near-real-time detection of asteroids using a new and very fast digital tracking approach. Once achieved, this objective could actually become, to the best of our knowledge, the first digital tracking pipeline developed in Europe. The novel algorithm and operation of the three main modules of the Umbrella suite are described in detail in a companion software paper (Stanescu et al. 2025, submitted).

In the present survey paper, we will briefly introduce our software suite and present its application to a few mini-surveys carried out with three survey telescopes between 2022 and 2024. In Section 2 we briefly introduce our Umbrella synthetic tracking suite. In Section 3 we present our NEA mini-surveys, and in Section 4 we list our results, sorting out the discoveries, co-discoveries, recoveries, lost (one-night) NEAs, and other related objects. In Section 5 we compare our STU detections and computing runtimes with those obtained by *Tycho Tracker* software. In Section 6 we compare survey limits using the traditional blinking with synthetic tracking, and in Section 7 we calculate NEA discovery statistics based on our surveys. In Section 8 we list the main conclusions of our ParaSOL survey work, planning some future work.

## 2. The Umbrella Synthetic Tracking Suite

Our Umbrella suite was developed during the ParaSOL project based on previous image reduction and blinking detection Umbrella code developed mainly by Malin Stanescu [52]. The aim of the Umbrella suite was to implement a synthetic tracking pipeline capable of reducing in near-real-time mini-surveys carried with large field-of-view telescopes. In this Section, we give a quick overview of the three modules of the Umbrella suite needed to process the survey fields which consists in series of at least 9 images needed to feed ST with three groups of at least three consecutive images. The full technical description of the Umbrella suite is given in a companion paper (Stanescu et al. 2025, submitted).

### 2.1. IPP Summary

To accommodate our tests and ParaSOL mini-surveys, we have developed the *Image pre-Processing Pipeline* (IPP) module aimed to perform corrections of the raw images taken by any instrument fully characterised in a configuration file. In general, IPP includes corrections due to the sensor electronics (bias, dark, bad pixel), telescope/instrument

<sup>19</sup><https://planet.astro.ro/ParaSOL>

optics (flat field and optical distortions), and in the future we plan to add crosstalk and bleeding corrections (which during our mini-surveys we have already applied via some dedicated Python/IRAF scripts).

## 2.2. STU Summary

Following our *Umbrella* blinking detection project, during 2021 Malin Stanescu has embarked in the development of the *Synthetic Tracking via Umbrella* (STU) module aimed at detecting faint moving sources. STU is a very fast implementation compared with other similar methods, leveraging GPU acceleration, a staged hypothesis rejection design (similar to the method used in [25]), as well as several search space optimizations and co-addition tricks to quickly scan wide fields for the fast moving objects.

The main aim of our ParaSOL project was the development of the *Synthetic Tracking on Umbrella* (STU), a fast ST module aiming to detect in real-time faint NEAs, satellites or space debris. STU adopts a staged hypothesis rejection design, leverages GPU acceleration and makes use of several search space optimizations and co-addition tricks to achieve real-time operation at NEO-level proper motion rates. STU was first announced in two conferences, namely the ACM 2023 [53] and the IAA PDC 2023<sup>20</sup>. Its technical description and few flowcharts are presented in the companion paper (Stanescu et al. 2025, submitted).

## 2.3. Webrella Summary

*Webrella* represents the online module needed to validate STU detections. During the ParaSOL project it has been re-written since its first version [52], due to the need to accommodate the new IPP pipeline (which was not envisioned in the first implementation of *Umbrella*) and to address some of the usability pitfalls of the first version.

## 2.4. STU Parameter Optimization

To improve STU detection rates, during the ParaSOL project we have searched for the optimal parameters for the detection algorithm. This search was conducted over all three parameterizable stages of STU, using archival data from our KASI mini-surveys which include 382 known asteroids.

First, GPU parameters were scanned automatically to characterize the behavior of the brute force scan, specially since it was noted that lower thresholds sometimes yielded less detections. This was followed by a semi-automatic multi-parameter scan of the third and fourth stages, by successively optimizing each parameter in turn until an acceptable ratio of true positives to false positives (16 true positives for 100 false positives) was achieved at the faintest level possible. This ratio was driven by the time available to our reducers to scour through the list of detections in near-real-time.

The parameter space of the GPU scan stage has shown a detection cliff at high apparent speed limits and low detection thresholds. This was correlated with an increase of the number of detections coming out of the GPU stage. In particular, when detection rates dropped to 1%, there was a detected vector coming out of the GPU stage for almost every pixel (90% of the pixels were part of a detection). Since STU has a second stage which pairs nearby pixels into detections, the loss of candidates is to be expected, as detections percolate into a giant single-candidate blob, which is swiftly rejected in the third stage.

Once the detection probability of each pixel crosses the site percolation threshold for  $\mathbb{Z}_2$  - approximately  $p \simeq 0.593$ , the random noise will begin to cluster in blobs [1], which do not exponentially decay, but rather obey a critical distribution, asymptotically a power law  $n_s \sim AS^{-\tau}$  (where  $\tau = 187/91$  is the Fisher exponent). This issue should be solved in a future version of STU, where the direction of the motion vectors will be considered in clustering detections. This will greatly lower the probability of random noise being clustered together, and thus eliminate noise percolation as a source of lost detections.

The result of the third stage optimization had normal behavior and has yielded a set of optimal parameters with 274 detected objects (out of 382, or 72%) and 1591 false positives.

<sup>20</sup>[http://www.euronear.org/publications/Stanescu\\_PDC2023.pdf](http://www.euronear.org/publications/Stanescu_PDC2023.pdf)

### 3. Applications

During the development of the ParaSOL project, we used the existing and upgraded Umbrella software suite (IPP, STU and Webrella), and also the *Tycho Tracker* software based on IPP output, aiming to employ our Umbrella software suite to discover and report NEAs and other asteroids in near-real-time.

A total of 10 observing runs were conducted within the time interval 2022-2024 using three survey telescopes, namely the *Isaac Newton Telescope* (INT - 4 visiting runs), the *Korean Astronomy and Space Science Institute* (KASI - 5 service runs) and the Brazilian T80S (one service run executed during a few nights). In Table 1 we show their features, namely: the telescope (acronym), location (acronym of major observatories), telescope diameter (in meters), focal over diameter ratio, camera, number of CCDs (for mosaic cameras), pixel size, pixel scale (in ″), field of view (FOV, in rounded arc minutes), *etendue* (in  $m^2 \text{deg}^2$ , calculated disregarding the central obstruction), and the MPC observatory code.

Following our past work [68], we define a regular *NEA candidate* as any unknown detection (not identified with any known asteroid but consistent with usual asteroid appearances) whose MPC NEO Rate score is above 50%. Also, following our earlier work [62] implemented later in our EURONEAR website as the NEA Checker Tool<sup>21</sup>, we define a *possible NEA candidate* as any unknown detection located above the magenta border in our elongation - proper motion ( $\epsilon - \mu$ ) model or clearly standing out among all other asteroids observed in the same field or region (either above the bulk, although below the border, or moving in a direction different from all the other asteroids on at least one of the  $\mu_\alpha - \mu_\delta$  or  $PA - \mu$  plots). The “magenta border” refers to the limit region between MBAs and NEAs as projected on the  $\epsilon - \mu$  plot, based on a simple model assuming a circular and coplanary-ecliptic orbit of a poorly observed unknown asteroid (during only one night) in possible recovery need due to its possible NEA candidacy. Because this border curve was drawn in magenta color [62], we continue to name it the “magenta border”.

To avoid NEA loss, during all our mini-runs we reported both possible and regular NEA candidates on “near-real-time” basis, usually defined as max 12 h after observations, attempting to reduce and report during the next day all fields observed during the previous night. To avoid false findings, most of the times we hold from submission some possible NEA candidates which could be artifacts, first attempting to recover them during the next night (if any such time was available). Nevertheless, when recovery was not possible, or when the day time was scarce to allow in depth analysis, rarely we submitted some NEA candidates which could be artifacts, and 4 such detections are included in this work. In this paper we include 59 possible and regular NEA candidates, presenting the observing circumstances of the most important detections, re-analyzing some difficult decisions, and classifying each candidate, before deciding which of them were actually artifacts, following careful analysis which was impossible to carry on during the mini-surveys.

Regarding the survey strategy, to increase discovery odds, we targeted fields not covered by major surveys during past week (based on the MPC Sky Coverage<sup>22</sup>), fields along or closer to the ecliptic, and higher in the sky. We planned to use STU with three co-adds, most of the time exposing 9 or 12 images with the INT and KASI, and 20 repetitions with T80S due to its smaller aperture. To avoid confusion with fixed sources, with the INT we allowed asteroids to move by cycling 4 neighboring fields (which added more overhead due to slew), but we took a series of 9-12 images in service mode with KASI and T80S which do not allow scripting.

#### 3.1. INT mini-surveys

A total of 382 fields (104 sq.deg) were surveyed during 100 hours spread across 23 nights (14 full visiting nights, plus other service time available for recoveries) of semesters 2023A, 2023B and 2024A using the 2.54-m *Isaac Newton Telescope* (INT) at *Roque de los Muchachos Observatory* (ORM) located at 2396 m altitude atop La Palma island. During the first and last part of most of these nights (about 3 hours per night), other fields were surveyed at low elongation regions part of another program targeting Atiras (PI: Raul de la Fuente Marcos), which are not included in this paper.

<sup>21</sup><http://www.euronear.org/tools/NEACheck.php>

<sup>22</sup><http://www.minorplanetcenter.net/iau/SkyCoverage.html>

At its  $f/3.3$  prime focus, the INT holds the *Wide Field Camera* (WFC), consisting of an L-shape mosaic of 4 CCDs of  $2048 \times 4200$   $13.5 \mu\text{m}$  pixels each (0.33 arcsec/pix) which cover in total 0.27 sq.deg. The resulting INT *etendue* is 1.37, which is feasible for some deep survey works (discovery and recovery), and during the past decade we used this facility for other related projects [62, 64, 66, 68].

With the INT we observed *ABCD* sequences, imaging neighboring fields (separated by  $40'$ ) to minimize the overhead and to allow time for slower asteroids to be detected. We used a Python TCS script to repeat 9 or 12 times each pointing (using 2-3" dithering to reject residual artifacts) exposing each image for 30 s or 45 s. Most fields were observed using  $9 \times 30$  s exposures, but we integrated longer during the brighter Moon periods and/or bad seeing conditions. The readout of the WFC in fast mode was 30 s, thus the effective time spent on sky during the INT mini-survey was less than half, due to many *ABCD* slews and change of fields. Only few of the fields targeted recovery of NEA candidates detected during past nights, and for some such fainter detections we used longer exposures (usually 60 s), repeating the field in only one position (A). Throughout our entire INT mini-survey we used tracking and Sloan  $r$  filter.

During the last few years, unfortunately the INT quality has degraded continuously (both in tracking and guiding modes), so specially during the last INT runs, we were affected by many telescope jumps during some exposures by a few pixels which resemble "double" or trailed stars. These problems affected the astrometry quality, reduction time and finally the number of INT detections, and during 2-3 nights the jumps affected as much as 30-40% of the images (ex. 20231101, 20240509).

The typical INT seeing was between 1.0-2.5" (average around 1.5") depending on the sky conditions (sometimes being affected by cirrus or clouds), the observed airmass and sometimes bad tracking. Thus, the INT seeing became about 2-3 times worse than the average ORM seeing (0.8") and above the average historic INT seeing (1.2").

The Moon was bright during the first INT run 20230227-0303 (only 5 hours dark time in total), mostly bright during the second run 20230410-11 (only 6 hours dark), during the observations of the few fields observed during the 20231018 service night (2 hours dark), bright during the third INT run 20231029-1104 (5 hours dark and run affected by bad weather for about half of time), dark during the fourth INT run 20240509 (5 hours dark and mostly affected by clouds during two nights), gray during the fifth INT run 20240528-31 and following few nights service (14 hours dark in total but affected by telescope jumps). Thus, from the total of 100 INT hours effectively observed, only 35 hours were dark (35%), while most others were bright.

In Table 2 we include the INT observing log, listing the observing date (start of the night, emphasizing in bold full visiting nights), number of observed fields, effective observed time (rounded hours), total number of known and unknown asteroids reported during each night, and the number of NEA candidates.

In Table 3 we report all INT NEA candidates, including our original name, designation (where available), orbital class (where available), the observing night (start of night, marking with "... " the same night), our field name (same convention), CCD number, number of individual images taken, exposure time (seconds), appearance (convention below), apparent magnitude (average of all reported positions), the position angle ( $PA$ ), proper motion ( $\mu$  in "/min), the Solar elongation ( $\epsilon$  in degrees), our NEA Checker status (acronym NEAC, convention below), MPC Digest2 NEO Rate (acronym NEOR, in percents), the acronym of the main reducer, total number of nights submitted ( $n$ , to reflect our recovery attempts), the actual status of detection (convention below), and the resulting MPC publications (where available: MPS and MPEC for discoveries, or ITF database for unpaired one-night detections).

In the first column of Tables 3, 5 and 7, nicknames in italic fonts represent detections missed by STU, those underlined mean detections missed by Tycho, while regular fonts refer to detections found by both software tools.

Throughout the paper, we adopt the following acronyms for the reducers: MP for Marian Predatu, OV for Ovidiu Vaduvescu, PO for Marcel Popescu, LC for Lucian Curelaru, MS for Malin Stanescu, and DB for Daniel Bertesteanu. Additionally to OV, MS and DB, 3 more INT observers attended 2 runs, namely: Costin Boldea (acronym CB), Felician Ursache (FU), and Corina Fotin (CF). Moreover, 6 ING students assisted some INT runs, namely: Freya

Barwell (acronym FB), Kiran Jhass (KJ), Shravya Shenoy (SS), Alejandro Santos (AS), Joshua Bishop (JB) and James Munday (JM).

Regarding the “Appearance” column, we adopt the following convention: *star-like* for clear regular detections (medium or brighter), *faint* for star-like faint detections, *fuzzy* for a few detections which look a bit extended (higher FWHM than usual), *limit* for detections at the limit of signal-to-noise (possibly artifacts), and *trail* (short or long) for clear trailing detections visible also in the original blink images.

Regarding the NEAC status based on our  $\epsilon - \mu$  model, we adopt the following notation: *clear* for detections located above magenta border in the  $\epsilon - \mu$  plot, *detached* for detections separated from the field bulk on at least one of the three plots (although possible below magenta), and *unclear* for usual detections not standing out on any of the 3 plots.

Regarding the “Status” column, we adopt the following convention regarding the detections: *discovery* when MPC lists the object initially reported or discovered from our site, *co-discovery* for objects reported by us almost simultaneously (few hours or days after the official discoverers with whom we share the same discovery publication), *recovery* for objects recovered following discovery or during second opposition (in which case we give the number of years, months or days not observed), *follow-up* for objects for which we improve the orbit with new data (at first, second or other opposition), *lost* for one night detections which could not be recovered (due to lack of time or visibility), or possibly *artifacts* at detection limit.

In Figure 1 we show the appearances of the NEA candidate detections observed with INT. For each detection we include all 3 co-adds found during the observing runs either by STU (when detected) or by Tycho (which STU could not find). We present each detection centered in a cropped field measuring  $33 \times 33''$ , marking STU detections with a red cross and Tycho findings with a red square. Stars are masked by the pipeline in case of STU detections, or they appear dimmed due to the median co-addition of sources in case of Tycho reduction. The background of Tycho images looks smoother compared with the STU images because of the different display options of the two software.

Besides our main aim to test the ability of the Umbrella software suite to detect NEA candidates, many known and other unknown asteroids have fallen in the observed fields of our mini-surveys, which became a by-product of our work, whose positions were reported to MPC in near-real-time, also serving in the quality control of the whole project.

Figure 2 shows the O-C residuals for all known asteroids reported to MPC observed with INT. We count 3195 known objects (according to the total included in Table 2), for which we submitted 8545 positions which appear in the plot, having a total root mean square error  $\sigma = 0.17''$  composed of  $\sigma = 0.21''$  on  $\alpha$  and  $\sigma = 0.16''$  on  $\delta$ . A clear elongation and small asymmetry around origin can be observed along the  $\alpha$  direction due to the known INT tracking and jumping problems.

### 3.2. KASI mini-surveys

A total of 142 fields (568 sq.deg) were observed in service mode during 62 hours in 11 nights (8 full service nights plus few hours granted for recoveries) of semesters 2023A and 2023B using the 1.60-m *Korean Astronomy and Space Science Institute* (KASI) Telescope located at *Cerro Tololo Observatory* (CTIO) at 2167 m altitude in the Chilean Andes. KASI celebrated its first light in September 2014 and is part of the *Korea Microlensing Telescopes Network* (KMTNet) which owns three identical telescopes at sites located in the South (Chile, South Africa and Australia) [36, 33].

At at the  $f/3.22$  prime focus, KASI is endowed with the *Korean Microlensing Telescope Network Camera* (KMTCam), which is a giant 341 Mpix mosaic comprising of 4 e2v  $9232 \times 9232$ ,  $10.0 \mu\text{m}$  pixels CCDs (pixel size 0.40 arcsec/pix) which cover in total 4 sq.deg effective (separated by  $6'$  gaps along RA and  $3'$  along DEC), generating a large *etendue* of 4.62, which is perfect for any survey works [4].

The readout time of the camera is about 90 s using 8 amplifiers and 32 readout channels generating in each of the 4 CCDs 8 vertical “stripes” of  $1211 \times 9232$  pixels and different bias levels. Since March 2022 stripe #23 has been broken, so the KASI covered area is actually 3.875 sq.deg. During our entire KASI survey, we used the Johnson-Cousins R

filter.

Due to very slow readouts, actually less than one third of the KASI time was spent on sky. To minimize slew time and due to service observations which are less flexible not allowing sequencing, for each field we used only one 10'' dithering in both  $\alpha$  and  $\delta$ , typically exposing series of 9 or 12 images (depending on the Moon) of 60 s each. For the recoveries of a few fainter NEA candidates we demanded 15-20 repetitions.

For unknown reasons, some of the KASI fields delivered less images, the minimum number of repetitions being 6 (instead of 9 demanded), while in other cases the telescope actually delivered one more image. In two cases it actually repeated the fields (delivering 24 instead of 12 images), and in one case the field was repeated 4 times, acquiring 51 images instead of the 9 demanded, which can be used for deep KASI statistics.

The typical KASI seeing was between 1.0-2.0'', usually about double than the average DIMM seeing in Tololo (0.8''), due to lower airmass and possible imperfect tracking (instead of guiding) and maybe imperfect optics across the very large field.

The Moon was dark during the first KASI run 20230216-18 (24 hours dark), bright during second run 20231022-23 (only 2 hours dark in total), dark during the second run (only 20231205 night) and few hours service recovery time (11 hours dark in total), dark during the third run (20240111 night 7 hours total), and again dark during the fourth run (20240210 night, 7 hours dark). Thus, from the 62 hours total effective KASI time, 51 hours were dark (82%).

Due to the large size of images (one raw image has 683 MB), the KASI image transfer was quite slow (with typical speeds of about 4-5 MB/s, sometimes slower) but the KASI staff kindly allowed nightly transfers of our data from CTIO soon after observations of each field, so that each typical field of 12 images (which spans 30 min and takes 8.2 GB) could be downloaded to our ParaSOL server in about the same time, good enough to allow near-real-time data reduction (on a daily basis).

The KASI image reduction was more difficult than for the INT and T80S, mainly due to the cross-talk and bleeding effects caused by the 8 amplifiers of the KASI very large 4 CCD mosaic camera, also due to the large size of the images; each typical field of 12 images needing about 60 GB total space to reduce, and 4 billion pixels to handle in the ST process. The KASI IPP image reduction module comprised 3+1 steps, explained below.

### 3.2.1. KASI Pre-Processing

First, we corrected the cross-talk effect using two C programs named *xtcoef* and *xtcorr*. These have originally been developed by Seung-Lee Kim (named *kmtnet\_xtcoef.c* and *kmtnet\_xtcorr.c*), being kindly provided by the KASI team [32]. To allow real-time data reduction, these programs have been further optimized for speed by the ParaSOL team and collaborator L. Stanescu.

In Figure 3 (see the online animated GIF<sup>23</sup>) we present an example of the cross-talk correction in a crop of CCD1 image *kmtc.20230217.004610.fits*, presenting the animation of the raw and cross-talk corrected image which fixes hundreds of artifact residuals generated by bright stars located in the neighboring CCDs or stripes (a few of them marked with green circles).

Second, we corrected each KASI image of bias and twilight flat (reduced from one master set taken each night), leveling the 8 stripes of each CCD (sometimes showing horizontal gradients) to the same flat background (common for each CCD), before splitting each reduced MEF image into 4 images (one for each CCD).

Third, for each CCD we corrected the bleeding effect by using the package *mscred* of IRAF (task *ccdproc*) with parameters carefully decided upon intensive testing before the first run, inspired also by the old manual *The Reduction*

<sup>23</sup><http://www.euronear.org/publications/Paper119-Fig3-KASI-cross-talk-animation.gif>

of *CCD Mosaic Data* of F. Valdes<sup>24</sup>. In Figure 4 (see the online animated GIF<sup>25</sup>) we present an example of bleeding correction in a crop of CCD4 image *kmtc.20230217.004598.fits*, presenting the animation of the raw and bleeding corrected image which fixes hundreds of residuals bright stars bleeding along CCD columns.

We used the bleeding correction only during the first run, before deciding to skip it during the other runs, because during the correction the flux of the cores of the brighter stars (responsible for the bleeding effect) become distorted (showing some “lines” clearly visible in the animated Figure 4). This bright star core effect confuses the source detection process which creates many false detections along the “horizontal” cores of each such brighter stars, so one needs another fancy tool to get rid of this correction effect, which we did not have time to develop during the observing runs.

### 3.2.2. KASI Field Correction

Finally, each of the 4 pre-processed CCD images were field corrected using our IPP SExtractor, Scamp and Swarp chain, taking into account Gaia catalog stars detected in the entire field of each  $1 \times 1$  sq.deg CCD. This field correction was quite small, but it was necessary due to the very large field of the camera. Thanks to the thousands of non-saturated catalog stars detected in each field, all CCD field distortion plots look like a quarter of a very round disk.

In Figure 5 we show such a distortion map (manually assembled from the 4 CCD plots) of the reduced image *kmtc.20231023.007739* in normal sky orientation (North up, East left). Although the optical field distortion pattern (plotted in colors) looks perfectly round, the 4 CCDs show imperfect alignment of the axes and small mis-matches of the corners, due to imperfect coplanarity and alignment of the CCDs.

In Table 4 we include the KASI observing log, listing the observing date (start of the night, emphasizing in bold full nights), number of observed fields, effective observed time (rounded hours), total number of known and unknown asteroids reported during each night, and number of unknown NEA candidates.

In Table 5 we report all KASI NEA candidates, using the same conventions as above. In Figure 4 we show the appearances of the NEA candidate detections observed with KASI. Each cropped field measures  $40 \times 40''$ . For 3 cases (*Mar0414*, *n3a5013*, *n5p5OV1*) STU could not find the detections in all 3 co-adds, in which case we present only 2 co-adds.

Figure 7 shows the O-C residuals for all known asteroids reported to MPC observed with KASI. We counted in total 18,952 known objects (acc to overall total included in Table 4), for which we submitted 48,012 positions which appear in Figure 5, having a total error  $\sigma = 0.16''$  ( $\sigma = 0.17''$  on  $\alpha$  and  $\sigma = 0.17''$  on  $\delta$ ). A perfectly circular spread of the cloud around the origin can be observed, proving the very good tracking and timing of the KASI telescope.

### 3.3. T80S mini-surveys

A total of 12 fields (24 sq.deg) were surveyed in service mode during 7 hours spread over 7 nights of semester 2023A, using the Brazilian 0.83-m T80S telescope located at *Cerro Tololo Observatory* (CTIO) at 2178 m altitude in the Chilean Andes. This telescope is devoted mainly for the *Southern Photometric Local Universe Survey* (S-PLUS), a project designed to cover 9300 sq.deg in 12 filters [39]. T80S saw first light in December 2014 and is the sibling of the Spanish T80-JAST telescope located at *Cerro Javalambre Observatory* which carries on the similar J-PLUS survey.

At its Cassegrain  $f/4.31$  focus, T80S is endowed with the large field camera T80Cam-S which uses one monolithic *e2V* detector of  $9232 \times 9216$ ,  $10 \mu\text{m}$ ,  $0.55''$  pixels, providing a field of  $1.4 \times 1.4$  deg (2 sq.deg), which gives an *etendue* of 1.0. During our mini-survey the camera had a readout time of 40 s and we used the Sloan *r* filter. The contribution of the flat field and bias is negligible, nevertheless we corrected for these effects.

<sup>24</sup><https://noirlab.edu/science/sites/default/files/media/archives/documents/scidoc1560.pdf>

<sup>25</sup><http://www.euronear.org/publications/Paper119-Fig4-KASI-bleeding-animation.gif>

Because T80S service operations can not accommodate scripting, during the T80S mini-survey we used 20 repetitions of 60 s images without any dithering. Throughout our mini-survey, the typical T80S seeing was within the range 1.0-1.5". During four nights (20230524, 20230526, 20230607 and 20230610), part of the quality control step, we remarked that O-Cs of the known objects were systematically shifted from origin, concluding that the telescope timestamp was affected by some unknown reason (between -9 and +35 s). Thanks to the many known MBAs (usually between 100-200) detected in each field, we could apply a correction to center the O-C cloud, fixing the timestamp problem before submission. The Moon was dark in all T80S fields (6.5 hours in total).

In Table 6 we include the T80S observing log, listing the observing date (start of the night), number of observed fields, the effective observed time (rounded hours), total number of known and unknown asteroids reported during each night, and the number of NEA candidates. In Table 7 we report all T80S NEA candidates, using the same conventions as above. In Figure 8 we show the appearances of the NEA candidate detections observed with T80S. Each cropped field measures  $55 \times 55''$ . For one case (Mar3769) STU could not find the detections in all 3 co-adds, in which case we present only 2 co-adds. Figure 9 shows the O-C residuals for all known asteroids reported to MPC of those observed with T80S. We counted in total 1281 known objects (according to the total included in Table 6), for which we submitted 3525 positions which appear in Figure 7, having a total error  $\sigma = 0.13''$  ( $\sigma = 0.16''$  on  $\alpha$  and  $\sigma = 0.14''$  on  $\delta$ ). A small elongation of the cloud suggests imperfect tracking, while the small deviation of the centre of the cloud relative to the origin proves a timing problem of the T80S telescope (mostly corrected in four of the seven nights).

## 4. Results

Based on Tables 3, 5 and 7, in the following sections we count the total number of discoveries, co-discoveries, recoveries, one-night, follow-up NEAs, and other related objects observed during the mini-surveys conducted with the INT, KASI and T80S telescopes.

### 4.1. NEA Discoveries

During all our mini-surveys we discovered and secured 5 NEAs (one with the INT and 4 with KASI), and below we will present their discovery circumstances.

Figure 10 shows the  $\epsilon - \mu$  plot for all valid detections found in the NEA candidate fields observed in our entire mini-surveys, drawing the INT findings in blue, KASI in red and T80S in green. The NEA candidates are marked as encircled points, while other regular detections are plotted with colored points.

#### 4.1.1. 2023 DZ2 (E309252)

After the publication of its first NEA Apollo orbit based on our three night data (MPEC 2023-F12<sup>26</sup>), 2023 DZ2 became a *Virtual Impactor* (VI), exciting international interest and global concern [41]. This discovery was possible thanks to near-real-time processing enabled by the software tools and infrastructure developed in the ParaSOL project led by PO, although its first validation was reported by CB using Tycho based on our IPP reduced images.

Baptized E309252, this NEA had a relatively bright magnitude ( $G = 20.1$ ) and a star-like appearance in the individual  $12 \times 45$  s INT images taken in the first NEA survey field (*n101*) of our entire survey. These observations were conducted during the first half of the first night of 27/28 Feb 2023 under gray Moon phase (57% of illumination). Adverse weather conditions impacted all major surveys during this period, which allowed us to target only fields along the ecliptic.

The entire INT run was observed by OV assisted by the former ING students FB and KJ. The images were promptly uploaded by OV to the ParaSOL server, being processed during the next morning (9 h from observations), when E309252 was detected by STU (Figure 3). The same source was also found independently by CB using Tycho based on IPP images as input, then confirmed by CB and DB using Astrometrica based on IPP-reduced images. The MPC report of CB was submitted during the beginning of the second night (21 h after observations) which allowed

<sup>26</sup><https://www.minorplanetcenter.net/mpec/K23/K23F12.html>

our immediate follow-up.

Based on the first night data, the NEOR model (rate 100%) and the NEAC model (circled point at  $\epsilon = 140.5$ ,  $\mu = 0.72$  in Figure 8) predicted a clear NEA status, so we prioritized *E309252* for recovery during the following available INT nights, which confirmed its status, the recovery data being submitted promptly to MPC (2 h from observations).

Following our first INT nights, we could predict a very low *Minimum Orbital Intersection Distance* ( $MOID = 0.000065$  au), with  $\sigma = 0.09''$  based on the 3-night orbit fitted with *Find\_Orb* software<sup>27</sup> (version 4 Jul 2022). This low  $MOID$  was soon confirmed independently by Carlos and Raul de la Fuente Marcos who suggested an origin of *E309252* in the Flora family region. Based on our later analysis of its long-term evolution orbit, we concluded that it will not impact Earth in the foreseeable future, thanks to secular near-resonant behavior controlled by Jupiter and Saturn [41].

This actual low  $MOID$  and almost zero inclination ( $i = 0.14918$  according to current MPC orbit) actually turned *E309252* into a VI, and based on our INT data alone we could predict a close approach with Earth on 25 March 2023 around 19 UT at a geocentric distance of 175,700 km (0.45 lunar distances) when *E309252* was predicted to reach an apparent magnitude  $V \sim 10$ . Actually, based on our initial INT photometry ( $H \sim 23.6$ ) and our three night orbit, we predicted the size of our VI between few dozen and about one hundred meters, which made *E309252* a possible Tunguska-size impactor.

Although the object was quite bright at discovery and became brighter, actually it remained unknown and unobserved for the next two weeks, which allowed some people to speculate about possible concealment by NASA due to a possible imminent impact<sup>28</sup>. Its late orbital MPC announcement was actually due to three circumstances. First, the bad weather prevented all major surveys (and other private surveys) to cover the sky and spot our object. Second, we submitted all our three MPC reports labeled as "NEA candidate" (instead of the correct "NEO CANDIDATE" keywords), so that *E309252* was never posted on the NEOCP, to be able to be announced and confirmed by others right after our discovery. Third, for some reason the MPC failed to link our submitted three nights, to be able to publish earlier our discovery. That is why its orbit was published two weeks following our run (on 20230316), after OV asked P. Veres at MPC about its status, who promptly responded and published MPEC 2023-F12 and MPS 1810607, which designated *E309252* = 2023 DZ2 as our first ParaSOL discovery (assisted by Tycho).

Soon after publication of 2023 DZ2, based on our 3-nights INT data alone, all three available impact monitoring systems (NASA/JPL Sentry<sup>29</sup>, NEODyS Clomon-2<sup>30</sup> and the ESA Aegis software feeding the ESA Risk List<sup>31</sup>) predicted our VI with possible impacts in 27 March 2026 with an *Impact Probability*  $IP = 1.3 \times 10^{-4}$  for Sentry,  $1.6 \times 10^{-5}$  for Clomon-2 and  $7.2 \times 10^{-6}$  for Aegis [18].

Following its discovery publication on 16 March 2023, other stations added new observations and improved the orbit, then Catalina, Pan-STARRS and Kitt Peak digged through their archives and could add precovery data which improved its orbit data-arc length from 18 to 62 days (albeit with some systematic errors in their right ascension positions). Then, many other stations added new observations, thanks to extended mass-media attention received due to an incoming near flyby on 25 March 2023 and non-null impact probability in 2026.

During the three weeks after our INT discovery, due to follow-up ground visual observations and radar data, the impact status evolved until 21 March 2023, when fortunately our 2023 DZ2 was eliminated from all three impact

<sup>27</sup>[https://www.projectpluto.com/find\\_orb.htm](https://www.projectpluto.com/find_orb.htm)

<sup>28</sup><https://theyflyblog.com/2023/03/jpl-confirms-billy-meier-prediction-about-dangerous-inbound-object>

<sup>29</sup><https://cneos.jpl.nasa.gov/sentry>

<sup>30</sup><https://newton.spacedys.com/neodys/index.php?pc=4.1>

<sup>31</sup><https://neo.ssa.esa.int/risk-list>

monitoring lists (cf. ESA/Aegis<sup>32</sup> and JLP/Sentry<sup>33</sup>), ending its 23 days life as a known Virtual Impactor.

Because of its incoming flyby in 25 March 2023 and followed by the possible impact in 2026, at least two major campaigns to observe the physical properties of 2023 DZ2 were rapidly engaged during its flyby. We present briefly their results.

First, we used three telescopes in Tenerife and La Palma to acquire physical data, namely the 0.80 m *Two-Meter Twin Telescope* (TTT) to resolve its lightcurve in a very fast rotation ( $P = 6.2743 \pm 0.0005$  min), the 1.5 m *Carlos Sanchez Telescope* (TCS) to acquire spectro-photometry, and the 10.4 m *Gran Telescopio de Canarias* (GTC) to observe its visible spectra which resulted an X-type taxonomic class with probable high albedo and we could improve its absolute magnitude to  $H \sim 24.3 \pm 0.4$ , decreasing the size within the range 33-55 m, calculated with an albedo range of 0.42-0.15 [41].

Second, only 10 days before its flyby, the IAU embarked in an international IAWN campaign which later confirmed the fast rotation, taxonomy and irregular shape of 2023 DZ2, based on worldwide data which included Goldstone radio observations [43]. This campaign confirmed our predicted irregular shape, also its fast rotation ( $6.2745 \pm 0.0030$  min) and high albedo (0.49, derived from polarimetric and thermal IR observations), which further shrinks its diameter to  $30 \pm 10$  m. Actually, this IAWN observing campaign focused on our former VI 2023 DZ2 was the sixth such IAU campaign<sup>34</sup> and the first one prepared and conducted in “real-time”, closely before and during the flyby of 2023 DZ2 on 25 March 2023.

The current observed arc of 2023 DZ2 is 73 days, and the next recovery opportunity will be 4 April 2026 ( $V = 19.1$ ,  $\sigma = 4'$ , flyby at a distance of 0.00696 au) observable starting from 20 January 2026 when magnitude will drop below  $V = 23$ .

#### 4.1.2. 2023 XC8 (*n3b3W02*)

This Amor NEA was discovered by PO using our Umbrella suite in the *n3b3* survey field observed during first half of night 5/6 Dec 2023 (dark time) with the KASI telescope. Moving with  $\mu = 2.51''/\text{min}$  and appearing as a short trail visible in each of the  $13 \times 60$  s images, it became a clear NEA candidate, being located above the  $\epsilon - \mu$  magenta border and having a NEOR of 100%. It was confirmed visually by OV using DS9 blink, then reported to MPC quite late (36 h after observations, due to massive amount of KASI data), and appeared on NEOCP. This detection was initially missed by Tycho (reduced by MP) due to a lower search limit, but it could be reproduced by Tycho later.

During that run, we had only one KASI night available (which was very productive, producing another six NEA candidates presented below), so we asked for short recovery time which the Korean team kindly granted during the next few nights, and we could recover *n3b3W02* first during the 8/9 Dec night (measured by DB with Tycho), then recovered again accidentally (while targeting another NEA candidate) during the 10/11 Dec night (validated by PO using Umbrella suite). Finally we secured three KASI nights and could confirm its NEA orbit, the object being reported independently by Catalina and the private survey of the *Astronomical Research Observatory, Westfield*. These data allowed the designation of the object as 2023 XC8, published in MPS 2072562 and MPEC 2023-X212<sup>35</sup>. Actually, 2023 XC8 became our first NEA discovered entirely with our Umbrella suite via synthetic tracking, and possibly the first NEA ever discovered with KASI.

The current observed arc of 2023 XC8 is 45 days (thanks to Pan-STARRS, Catalina, and other Cerro Tololo observations),  $MOID = 0.07201$  au,  $H = 24.99$  resulting in a size within the range 20-40 m (assuming an albedo between 0.1-0.5). Its next recovery opportunities will be Jan 2027 ( $V = 20.8$ ,  $\sigma = 4^\circ$ ), Dec 2029 ( $V = 21.1$ ,  $\sigma = 7^\circ$ ) and Dec 2032 ( $V = 21.2$ ,  $\sigma = 13^\circ$ ), according to *Find\_Orb*.

<sup>32</sup><https://neo.ssa.esa.int/search-for-asteroids?sum=1&des=2023DZ2>

<sup>33</sup><https://cneos.jpl.nasa.gov/sentry/removed.html>

<sup>34</sup><https://iawn.net/campaigns.shtml>

<sup>35</sup><https://www.minorplanetcenter.net/mpec/K23/K23XL2.html>

#### 4.1.3. 2023 XV21 (*n3c1093*)

This Apollo was discovered in the *n3c1* field observed with KASI during the same night 5/6 Dec 2023 (dark time before the morning gray Moonrise), being validated by MP using Tycho based on our own IPP reduced images. Moving with  $\mu = 1.63''/\text{min}$ , it was detached on the  $\epsilon - \mu$  plots with NEOR 93%, appearing as a quite faint  $G = 20.8$  star-like detection in the 3 co-adds from  $26 \times 60\text{s}$  images reported 31 h after discovery.

Thanks to the same KASI directorship discretionary time, soon after discovery we could use KASI to recover *n3c1093* during two nights (8/9 and 10/11 Dec 2023), confirming the NEA status of 2023 XV21, which was published in MPEC 2024-A06<sup>36</sup> and MPS 2079759.

According to MPC current data of 2023 XV21, its MOID is 0.05441 au, and its absolute magnitude  $H = 23.63$ , which translates in a size range of 40-80 m (assuming an albedo range of 0.5-0.1). Its orbital arc is only 41 days (thanks to independent follow-up observations by *Mount John Observatory*, *Lake Tekapo* and *Cerro Tololo*). Although the uncertainty is growing, the next recovery opportunities will be: Sep 2027 ( $V = 23.8$ ,  $\sigma = 25'$ ), Aug 2031 ( $V = 23.3$ ,  $\sigma = 55'$ ), Oct 2034 ( $V = 23.3$ ,  $\sigma = 2^\circ$ ) and May 2035 ( $V = 22.4$ ,  $\sigma = 5^\circ$ ) - brightest but most uncertain.

#### 4.1.4. 2023 XP14 (*n6p5W04*)

This Apollo NEA was discovered by LC using STU in the *n6p5* field observed with KASI during the dark night 10/11 Dec 2023. Moving quite fast ( $\mu = 4.65''/\text{min}$ ), it appeared as a quite bright small trail (we estimated by eye  $G \sim 20$ ) in all  $15 \times 60\text{s}$  images, which made it a clear NEA candidate for both NEOR and our  $\epsilon - \mu$  model. We have confirmed it both with Tycho and visually with blink, reporting it 29 h after observation, when it appeared on the NEOCP. Apparently it was observed two nights before by Catalina, but they either reported it late or actually could precover our NEOCP detection.

As we could not get any more time from KASI, OV asked some EURONEAR collaborators for recovery. This succeeded, so that *n6p5W04* was confirmed during the next nights by ESA-OGS 1 m in Tenerife, Calar Alto-Schmidt 0.8 m, and the 1 m telescope at *Zadko Observatory*, *Wallingup Plain in Australia* - all thanks to ESA (Marco Micheli), and Cerro Tololo (thanks to Tyler Linder). Finally, 2023 XP14 was published in MPEC 2023-X310<sup>37</sup> and MPS 2072578. Thanks to KASI extended team who awarded us some time for recovery in their KASI SAAO site, but the seeing was very poor there and the pointing could be off.

According to MPC, the current orbital arc of 2023 XP14 is 125 days. Its  $H = 22.38$ , which results in a size range of 60-140 m (assuming albedo between 0.1-0.5). The next visibility windows will be: Aug 2028 ( $V = 24.4$ ,  $\sigma = 6'$ ), Nov 2032 ( $V = 22.9$ ,  $\sigma = 23'$ ) and Mar 2033 ( $V = 21.8$ ,  $\sigma = 46'$ ).

#### 4.1.5. 2024 AZ10 (*n7b3211*)

This Apollo NEA was discovered by MP using Tycho based on our own IPP  $10 \times 60\text{s}$  reduced images observed by KASI during the dark night 11/12 Jan 2024. Nevertheless, its possible NEA candidature status remained unknown during next months. It was detected promptly (next day) by MP as a faint ( $G \sim 22$ ) star-like appearance in the co-added Tycho images, being confirmed much later by OV in DS9 blink images, as a common asteroid moving quite slowly ( $\mu = 0.49''/\text{sec}$ ).

Following quality control and reporting steps, the appearance of *n7b3211* did not attract our attention, because its location remained unclear in our main  $\epsilon - \mu$  plot (not standing out among the bulk on the main plot, although was a bit isolated on the other two  $\mu_\alpha - \mu_\delta$  and  $\mu - PA$  plots), and having NEOR of only 12%, OV reported *n7b3211* as a regular asteroid (64 h after observation), so that our report was not posted on NEOCP, but ended temporarily in the ITF database.

Fortunately, *n7b3211* was on a brightening course during the next days, and its case was probably re-checked one week later by the MPC automated pairing system, following independent recoveries one week later by Pan-STARRS ( $G = 20.7$ ,  $\mu = 1.1''/\text{min}$ , NEOR of 45%) and ATLAS survey ( $\sigma = 18.5$ ,  $\mu = 6.5''/\text{min}$ ) which boosted their NEOR to

<sup>36</sup><https://www.minorplanetcenter.net/mpec/K24/K24A06.html>

<sup>37</sup><https://www.minorplanetcenter.net/mpec/K23/K23XV0.html>

100%, which posted it on NEOCP, after which many other stations could follow-up.

We found our discovery publications eight months after the run, thanks to the MPC WAMO tool, after OV revised some pending detections, then we could trace our discovery of 2024 AZ10: MPEC 2024-C39<sup>38</sup> and MPS 2117466.

The current arc of 2024 AZ10 is 39 days,  $MOID = 0.0683$  au and  $H = 22.54$ , resulting in a size range of 60-130 m. Next visibility opportunities will happen more often but detection remains quite shallow: Dec 2025 ( $V = 23.2$ ,  $\sigma = 7'$ ), Aug 2027 ( $V = 23.9$ ,  $\sigma = 10'$ ), Jan 2029 ( $V = 23.7$ ,  $\sigma = 15'$ ), Jan 2031 ( $V = 23.6$ ,  $\sigma = 27'$ ), Sep 2032 ( $V = 23.6$ ,  $\sigma = 33'$ ). Nevertheless, we proved that 2 m class telescopes could conduct recovery observations above  $V = 23$  [66].

## 4.2. NEA Co-Discoveries

We discuss in this section NEA candidates unknown at the time of our reporting, which became co-discoveries due to other stations which observed and reported them shortly before our submission, for which we actually contributed and share the orbit publication. Three such NEAs were co-discovered during our mini-surveys, one with the INT and two with KASI.

### 4.2.1. 2024 JJ25 (*n4b3169*)

This Apollo NEA was hoped to become our discovery, mainly due to its NEOCP posting for about 6 hours, but one day later it was credited to Pan-STARRS which actually observed it first, 27 days before us.

Nicknamed *n4b3169*, it was detected by MP using Tycho right after midnight on 28/29 May 2024 (dark time) in the *n4b3* field observed with the INT by MS assisted by the ING student JB and remotely by OV. It showed as a star-like, quite bright  $G = 19.3$  detection, visible in both the co-added and individual  $9 \times 30$  s images. During our quality control step, no identification could be made with any known asteroid using the *MPChecker* tool (searched in a radius of  $60'$ , for more safety).

Moving with  $\mu = 1.05''$  at  $\epsilon = 158.0^\circ$ , *n4b3169* has fallen clearly detached and above the  $\epsilon - \mu$  magenta border, moreover its NEOR of 93% made it a clear NEA candidate, so OV reported it during the next evening (on May 29.78 UT, 19 h after observations), when it was posted on NEOCP. We could recover it promptly during the second evening of our INT run, then we reported promptly (4 h after observations).

Although we hoped to secure our new NEA discovery due to its publication on NEOCP, we believe the crediting process of *n4b3169* remains a bit confusing, possibly due to delayed MPC pairing with older Pan-STARRS observations, or maybe due to (some) precoveries of Pan-STARRS in their older coverage, possibly triggered by our own *n4b3169* NEOCP publication.

Soon after our NEOCP posting, MPC updated the observations of *n4b3169* with Pan-STARRS coverage made 7 h after our own. Few hours later, a new set of Pan-STARRS observations (made 20 days before us) showed on the updated NEOCP data, then object disappeared from the NEOCP (soon after midnight of 29/30 May), so the suspense continued. During the next morning, the MPC observations database updated with three more Pan-STARRS dataset (observed 21, 23 and 27 days before us) and the discovery credit went to Pan-STARRS.

Finally, our NEA candidate *n4b3169* was published as 2024 JJ25 in MPS 2179354 and MPEC 2024-K132<sup>39</sup>, crediting Pan-STARRS as initial reporters, but having our INT submission (plus four other stations) sharing the same discovery publication.

Having a current orbital arc of 162 days (thus, quite accurate orbit),  $H = 22.44$  (size probably within the range 60-140 m), and a safe  $MOID = 0.02268$  au, 2024 JJ25 will remain quite scarcely visible in the future: very faint in Mar 2028 and Nov 2031 ( $V \sim 25$ ), but observable in Sep 2035 ( $V = 21.7$ ,  $\sigma = 1.5^\circ$ ).

<sup>38</sup><https://www.minorplanetcenter.net/mpec/K24/K24C39.html>

<sup>39</sup><https://www.minorplanetcenter.net/mpec/K24/K24KD2.html>

#### 4.2.2. 2023 XA3 (*n3b3W01*)

This Apollo NEA was seen first by PO using our Umbrella suite during the dark time of the night 5/6 Dec 2023 in the *n3b3* field observed with KASI. Moving very fast ( $\mu = 7.82''/\text{sec}$ ), it appeared as a quite faint long trail, estimated visually at  $G \sim 21.2$  in all  $13 \times 60$  s images. This STU detection was missed by Tycho (reduced by MP), due to the limit  $\mu \sim 2''/\text{min}$  which we needed to set in Tycho to reduce faster all KASI images, but it could be confirmed later when we restrained the search (by constraining the  $\mu$  and  $PA$  intervals) to be able to reproduce it. To facilitate its recovery (due to very fast motion and growing uncertainty), OV measured carefully its positions (middle of trails) in all individual images, then he reported the findings (35 h after observations).

During the following hours, unfortunately our *n3b3W01* detection did not show on NEOCP. It was probably in the pairing process of MPC, taking into account other coverage provided by Pan-STARRS (17 h before and 6 h after us) and Catalina (2 h after us), then again by Catalina and Pan-STARRS (all after our reporting), which added 3 nights data. Finally, 2023 XA3 was credited to Pan-STARRS, being published in MPEC 2023-X123<sup>40</sup> and MPS 2057153.

Because of its very short orbital arc of only 3 days, future recovery of 2023 XA3 will remain improbable due to its faintness: Mar 2026 ( $V = 28.9$ ,  $\sigma = 23'$ ), May 2028 ( $V = 29.0$ ,  $\sigma = 42'$ ), Jul 2030 ( $V = 27.7$ ,  $\sigma = 2.1^\circ$ ), Mar 2033 ( $V = 28.6$ ,  $\sigma = 1.8^\circ$ ), while its past close approaches were in Dec 1979 ( $V = 27.8$ ,  $\sigma = 10^\circ$ ) and Oct 2016 ( $V = 25.6$ ,  $\sigma = 15^\circ$ ), so precovery is impossible, and thus, in practice 2023 XA3 could be considered lost. Fortunately, with  $H = 27.32$ , 2023 XA3 is quite small (probably having a size within the range 5-15 m), with  $MOID = 0.00859$  au, and thus it was never included in any VI lists, and our KASI data contributed to eliminating its potential threat.

#### 4.2.3. 2023 XN12 (*n6p2018*)

This Apollo NEA was validated by MP using Tycho in the field *n6p2* observed with KASI during the dark night 10/11 Dec 2023, during a short slot granted for recovery of another NEA candidate. It was moving with  $\mu = 2.11''/\text{min}$  which appeared as a quite faint ( $G = 21.5$ ) slightly elliptical detection in the three Tycho  $13 \times 60$  s co-added images.

Due to its higher speed, *n6p2018* appeared remarkable on the  $\epsilon - \mu$  and the  $\mu_\alpha - \mu_\delta$  plots, and had a NEOR of 100%, so it was reported as a NEA candidate (14 h after observations), following some careful scrutinizing of OV of the individual images, in which it was barely visible. Following submission, it did not show up on NEOCP, being paired later with another candidate observed by both Pan-STARRS telescopes 3-6 nights before us. Finally, 2023 XN12 was credited to Pan-STARRS and published in MPEC 2023-X270<sup>41</sup> and MPS 2072573.

This NEA does not present any risk, due to its relatively high MOID of 0.07188 au, its absolute magnitude  $H = 23.45$  suggests a probable size range of 40-90 m. Thanks to follow-up of Spacewatch six days after our co-discovery, the orbital arc became 12 days, allowing to predict that 2023 XN12 will remain extremely faint in the future (mostly  $V > 26$ ) with the first recovery opportunity in June 2038 ( $V = 22.0$ , with large uncertainty  $\sigma = 15^\circ$ ) and no other precovery odds (in May 1985 and Nov 2006), due to huge uncertainties.

### 4.3. One-night NEA Discoveries

In this section we discuss NEA candidates clearly detected in the co-added images and visible in each individual image, appearing as trails due to their faster proper motion, which have been observed during one night only. During our mini-surveys, we have discovered 4 such one-night NEAs (2 with the INT and 2 with KASI), which became lost due to lack of time for recovery or very late reduction. Their reported positions, blinked and co-added detection images are included on the EURONEAR Discovery page<sup>42</sup>.

Precovery or recovery should be attempted for our one-night objects when image archives will become available, specially searching the Pan-STARRS and Catalina surveys (which apparently covered some of our fields) and maybe other surveys which observed close in time (about one week) to our fields.

<sup>40</sup><https://www.minorplanetcenter.net/mpec/K23/K23XC3.html>

<sup>41</sup><https://www.minorplanetcenter.net/mpec/K23/K23XR0.html>

<sup>42</sup><http://www.euronear.org/discoveries.php>

#### 4.3.1. *n5b7402*

The clear NEA candidate *n5b7402* was detected two weeks later by OV using Tycho, in the *n5b7* field observed with the INT during the night 29/30 May 2024 (dark time) by observers MS assisted by the ING student JB and remotely by OV. Our STU software has detected it soon after the run, but unfortunately the team did not validate sooner this field. This object was moving fast ( $\mu = 7.09''/\text{min}$ ), being detected as a small trail later in the co-added images (using both Tycho and STU) and was clearly visible in each of the  $9 \times 30$  s images at  $G = 20.8$ . Due to its fast proper motion, *n5b7402* became a clear NEA candidate in our  $\epsilon - \mu$  model, and had a NEOR = 100%. OV found it first with Tycho, then PO found it in the STU folder, unfortunately not validated earlier. We reported it 13 days later, when it was posted on the NEOCP for a few days, then it had been moved to the ITF one-night database, probably after nobody else dared to attempt its recovery due to huge positional uncertainty.

#### 4.3.2. *n6c2188*

This clear NEA candidate was detected by MP using Tycho in the *n6c2* based on IPP images observed with the INT during the night 30/31 May 2024 (dark time) by MS, assisted on site by the ING student SS and OV remotely. It was moving with  $\mu = 2.50''/\text{min}$  through a relatively dense star field. It appeared quite faint ( $G = 20.2$ ) and fuzzy star-like (due to poor seeing  $FWHM = 1.9''$ ) and it could be confirmed later with STU, being barely visible in the  $9 \times 30$  s individual images and probably a miss for blink software.

Located above the  $\epsilon - \mu$  border and having a NEOR of 97%, *n6c2188* became a clear NEA candidate, but it was confirmed very late by DB and OV who reported to MPC 13 days after observations, after which it was posted on the NEOCP for a few days, then moved to ITF database.

#### 4.3.3. *n3b1W01*

This clear NEA candidate was detected by OV using the entire Umbrella suite (IPP, STU and Webrella) as a small trail with ParaSOL STU in the *n3b1* field observed with KASI during the night 5/6 Dec 2023. It appeared quite faint (estimated visually at  $G \sim 20.0$  in the individual images) and was moving quite fast ( $\mu = 5.48''/\text{min}$ ), and it could not escape to STU (being also confirmed by Tycho later), but it was probably a miss for blinking software. Due to its high proper motion, it stood out on the  $\epsilon - \mu$  plots and had a NEOR of 100%, so we submitted the report as a NEO candidate (32 h following observations), then it was posted on NEOCP for a few days.

Thanks to some very short KASI director time available two nights later (7/8 Dec 2023), we attempted to recover *n3b1W01*, when its uncertainty predicted by Find\_Orb and MPC NEOCP reached about  $\sigma = 7^\circ$ . We asked for 5 pointings covering along the uncertainty path, from which KASI could only cover two, but unfortunately no recovery candidate fallen in any of these, after careful search of PO with STU and MP with Tycho software. Other requests for recoveries from other stations could not produce any other results, and we thank M. Micheli and T. Linder for attempting to save our NEA.

#### 4.3.4. *n6p3W06*

This clear NEA candidate was detected by LC using the entire Umbrella suite as a small trail in the *n6p3* field (aimed during DDT granted for recovery of other seven NEA candidates), observed with KASI during the dark night 10/11 Dec 2023. It appeared as a faint ( $G = 21.5$ ) small trail clear STU detection in three co-added STU images, being also caught later by Tycho and barely visible in each of the  $20 \times 60$  s individual exposures (but probably missed by other blinking software).

Due to its fast proper motion ( $\mu = 4.06''/\text{min}$  and NEOR 100%, it became a clear NEO candidate, being submitted to MPC 53 h after observations, when it was posted on NEOCP for a few days. Unfortunately, no KASI DDT was available during next nights, and no other collaborating station could follow-up anymore, so that *n6p3W06* became our fourth ParaSOL one-night NEA discovery, currently in the ITF database.

### 4.4. Other Related Discoveries

During the recovery and follow-up process of some NEA candidates (all included in Tables 3, 5 and 7, we discovered 5 orbitally related NEAs, namely Hungaria and Mars Crossing asteroids (MC), whose circumstances we brief here.

#### 4.4.1. Hungaria Discoveries

Three Hungaria asteroids were found by our team, two with the INT and one with KASI.

2023 VG4 (*KA01044*) was discovered by PO using the Umbrella suite in INT images observed during the night 2/3 Nov 2023 by CB and FU, who could recover and follow-up the object during 3 nights. Soon after our common submission, it was probably precovered in Pan-STARRS archives (2022, 2017 and 2015), then followed from Kitt Peak and Catalina, being published in MPS 2034097.

2024 KL8 (*N6B6W01*) was discovered by MS using our Umbrella suite in INT images observed in the night 30/31 May 2024 by MS assisted onsite by ING student SS and remotely by OV. It appeared star-like and quite faint ( $R = 22.2$ ) in the STU co-added images, being probably missed by any blink detection software. It was moving moderately ( $\mu = 1.07''/\text{min}$ ), being located above our  $\epsilon - \mu$  border but a low NEOR of 10%. It was submitted as a possible NEA candidate (after 18 h) and next nights it was recovered with the INT, being followed one month later by Pan-STARRS. It was published in MPS 2201381 and has a current arc of only 32 days.

Nicknamed *n3b4079*, this NEA candidate was validated by MP using Tycho based on IPP reduced images, as a star-like quite faint  $G = 20.4$  co-added detection observed with KASI during the night 5/6 Dec 2023. It was moving moderately ( $\mu = 0.98''/\text{min}$ ) but appeared detached from the bulk in two of our  $\epsilon - \mu$  plots and had a NEOR 84%, so it was submitted as a NEA candidate (after 36 h, following careful checking), being posted on the NEOCP, but nobody could recover it. Only five nights later (dark night 10/11 Dec with good seeing  $1.0''$ ), we could use again KASI to confirm it, after careful comparison of both datasets. Thus, we could link a 2 nights orbit ( $\sigma = 0.08''$ ), which makes *n3b4079* a probable Hungaria, according to *Find\_Orb* ( $a \sim 1.8$  au,  $e \sim 0.1$ ,  $i \sim 20.6^\circ$ ,  $q \sim 1.7$  au, albeit with large uncertainties). Currently both nights remain still in the ITF database (strangely un-linked by MPC), so that *n3b4079* did not receive any designation yet. Thanks to Tylor Linder (CTIO) and Javier Flores (Calar Alto) who attempted its recovery, the object remaining probably fainter than their capabilities.

#### 4.4.2. Mars Crossing Discoveries

We probably discovered two Mars Crossing asteroids (MCs), one with T80S and another with KASI.

2023 MD1 (*Mar3769*) was validated by MP using Tycho based on IPP reduced images observed during the night 15/16 Jun 2023 in service mode with T80S telescope. Later it was confirmed by OV using STU which detected only two co-adds (presented in Figure 8) based on the same  $20 \times 60$  s dataset. Moving with only  $0.76''/\text{min}$ , it appeared as a faint  $G = 20.4$  star-like detection, probably missed by blinking software. Its location was detached (about twice above) from all other objects, and it had a NEOR of 90%, so it was submitted as NEO candidate (36 h after observations). It was posted on NEOCP and could be recovered twice by T. Linder with the CTIO 1 m telescope, then recovered by Pan-STARRS, Spacewatch, and later followed-up and precovered by Catalina and Pan-STARRS. Our 2023 MD1 discovery was published in MPS 1894649.

2023 XB44 (*n5p3001*) was validated by MP using Tycho in a recovery field observed with KASI during the night 8/9 Dec 2023, being confirmed later by OV using STU (detection included in Figure 6). It had a star-like regular  $G = 20.0$  appearance, moving moderately ( $\mu = 0.75''/\text{min}$ ) which made its NEA candidature status unclear on our NEAC plots compared with few other objects detected, but its NEOR was 72%, which targeted recovery using again KASI which succeeded two nights later, our discovery being published in MPS 2267050.

#### 4.5. Other Related Co-Discoveries

A total of 7 Hungaria, Mars Crossing (MC), Phocaea and Main Belt asteroids (MBAs) were co-discovered by our team, one with the INT and four with KASI. They were discovered by other surveys shortly before our observations or reporting, but we share the same discovery publications. All these objects have appeared as NEA candidates (for at least one of the checking models) based on our first night data. During their chasing process, independently of discoverers or other stations, we could recover (observed in 2 nights - included as “2n” in the Tables) or follow-up some of these objects (observed in 3 nights - “3n” in the Tables).

#### 4.5.1. *Hungaria Co-Discoveries*

2023 BE16 (*Mar0262*) was validated by MP using Tycho in the INT images observed in the night 1/2 Mar 2023 by OV and ING students FB and KJ. It appeared star-like and quite faint ( $G = 21.0$  and almost invisible in the third coadd). Moving with  $\mu = 0.73''/\text{min}$ , it was a possible NEA candidate in our  $\epsilon - \mu$  plot but had a NEOR of only 11%. It was discovered by Pan-STARRS 40 days before us but linked later to Catalina and our independent data, being published in MPS 1916342.

2021 JD70 (*Mar0414*) was validated by MP using Tycho in co-added images observed during the night 17/18 Feb 2023 with KASI, being confirmed later by OV in two STU co-adds (included in Figure 6). It appeared as a star-like quite faint  $G = 20.7$  detection moving with  $\mu = 1.03''/\text{min}$ , becoming a possible NEA candidate based on its clear location above our  $\epsilon - \mu$  border and twice above the bulk formed by a very reach field which included 270 detections, nevertheless its NEOR was only 19%. We have reported it as a possible NEA candidate (after 22 h). This object was seen during our first KASI run, when we targeted the same fields during all three nights. It was detected during all three nights, but the first and the third nights were sent few months later as 2023 BE16, after it was linked and credited to Pan-STARRS. We co-discovered 2023 BE16 thanks to our rapid submission of our second night data, and we share its co-discovery and publications MPS 1747047 (published after discovery) and 1958994 (published months later, after our late submission).

2023 TH198 (*n1b1366*) was detected by MP using Tycho in KASI images observed during the night 22/23 Oct 2023, being later confirmed with STU by OV (whose detection we include in Figure 6). It appeared as a very faint star-like detection  $G = 23.5$  moving relatively slowly ( $\mu = 0.62''/\text{min}$ ), having unclear NEA candidature status based on NEAC and NEOR (only 11%), but we reported it in the batch of some possible NEA candidates. It was also detected by KASI during the next night (thanks to field repetitions of this second KASI run) and reported (but not paired). It was linked much later by MPC in the Hungaria orbit of 2023 TH198, and our 2n KASI data share discovery with one night Pan-STARRS which detected it 9 nights before us and then recovered it two months after us, all data being published in MPS 2254292.

#### 4.5.2. *Mars Crossing Co-Discoveries*

2022 XP8 (*Mar0817*) was validated by MP using Tycho in KASI images observed during the night 17/18 Feb 2023. It appeared star-like moderately faint ( $G = 21.7$ ), moving with  $\mu = 1.07''/\text{min}$  being located clearly above the  $\epsilon - \mu$  border (peaking and twice above all other 275 detections in that field), but having a modest NEOR 12%, so it was submitted as possible NEA candidate. This detection was paired with another unknown in our first KASI night. Both of our nights were paired by MPC in the MC orbit of 2022 XP8, observed by Catalina 5 days before us, and first by Pan-STARRS in 2022, which later added precovery data from 2015, our data being published in MPS 2056838.

#### 4.5.3. *Phocaea Co-Discoveries*

2023 TA174 (*n1a9328*) was reported by MP using Tycho during the KASI run Oct 2023 when KASI repeated some pointings. It was detected during both nights as a star-like appearance  $G = 20.2$  moving with  $\mu = 0.70''/\text{min}$ . Its location remained unclear in both NEAC and NEOR (22%), nevertheless it was submitted by PO as a NEO candidate. Later *n1a9328* was linked by MPC with two nights data of Pan-STARRS observed few days before us, our co-discovery of this Phocaea family object, 2023 TA174, being published in MPS 2093639.

#### 4.5.4. *Main Belt Asteroids Co-Discoveries*

Two main belt asteroids (MBAs) were co-discovered during the NEA candidate chasing process, both using KASI.

2023 RE156 *n1a4704* was detected by MP using Tycho in KASI images taken during the night 22/23 Oct 2023. It appeared as a star-like  $G = 20.4$  detection moving with  $\mu = 1.12''/\text{min}$  located detached on the  $\epsilon - \mu$  plot (on top and detached of the bulk of 10 objects detected in that field), and had a NEOR 36%, thus it was submitted as a possible NEA candidate. Later it was paired by MPC with other Pan-STARRS detections observed before us, also to another Pan-STARRS set of two nights observed in 2014. The object was designated 2023 RE156 (turned an inner MBA with  $a = 2.0$  au) and we share with Pan-STARRS its discovery published in MPS 2117400.

2023 TG143 (*n1b1361*) was detected by MP using Tycho in KASI images observed in the same night 22/23 Oct 2023, being confirmed later with STU (whose images we include in Figure 6). It appeared as a star-like  $G = 20.4$  moving with  $\mu = 0.55''/\text{min}$  whose location remained unclear on the NEAC and having NEOR 34%, but we decided to submit in a batch including some possible NEA candidates. It was designated as the MBA 2023 TG143, paired with two nights Pan-STARRS data (which hold the discovery status, because the first set was observed 9 days before us), being later precovered to a Kitt Peak 2022 detection. We share this co-discovery published in MPS 2057007.

Probably other MBAs were co-discovered or discovered in our survey, more probably during the first Feb 2023 and second Oct 2023 runs (when we repeated the pointings), but we did not attempt to pair and evidence them.

#### 4.6. Other One-Night Related Candidates

During our mini-surveys, we have evidenced and submitted 21 possible NEA candidates, all having only one-night data and star-like aspects, 17 of them being clearly detected with KASI and 4 which could be possible artifacts (two observed with KASI and two with T80S). Their observed circumstances and NEA candidacy status are included in Tables 3, 5 and 7, so we only list them below.

The 17 possible NEA candidates KASI detections with clear star-like appearances are: *n3o4081*, *n3o4097*, *n1e8new*, *n1a9326*, *n1b1362*, *n1b1363*, *n1b1364*, *n1b1365*, *n1b1367*, *n3c1087*, *n3c1088*, *n3c1089*, *n3c1092*, *n3c2067*, *n5p1107*, *n7a1206*, and *n7a2416*. The other 4 lower SN detections possible artifacts are: *n3o4089*, *n3a4018* (KASI) and *Mar3087*, *Mar3103* (T80S). All these reports are included in the ITF database (Nov 2024), but some could be later linked by MPC and “promoted” as co-discoveries or maybe our discoveries.

#### 4.7. NEA and Other Recoveries

In the process of chasing our NEA candidates detected in our mini-surveys, we recovered 3 known NEAs and other 8 known related NEA candidates at their first or second opposition. Their observing data are included in the Tables, and we present below their circumstances.

##### 4.7.1. NEA Recoveries

2021 PF10 (*n3c2066*) is an Amor NEA recovered at second opposition by MP using Tycho in KASI co-added images. appeared star-like and quite faint ( $G = 22.5$ , probably missed by other blinking software), moving with  $\mu = 0.83''/\text{min}$  and with NEOR 92%. It seemed unknown, so we reported it as a NEA candidate (albeit 12 days later). Our recovery happened two years since its discovery by Pan-STARRS, when its orbit had only one-month arc and therefore larger uncertainty ( $21'$ ), being published in MPEC 2024-B07<sup>43</sup> and MPS 2093525.

2023 QS3 (*n5p50V1*) is another Amor NEA recovered by OV (by chance visually) in KASI images, being confirmed later with STU in only two co-adds (see picture in Figure 6), and later with Tycho. It was moving faster ( $\mu = 2.31''/\text{min}$ ) showing a faint small trail (estimated visually  $G = 21.0$ ) with clear NEO candidature, which we reported 38 h later. The object was paired with NEA 2023 QS3 ( $\sigma = 3'$ ) discovered few months later of its Pan-STARRS discovery, so we prolonged its orbit from only 3 days to almost 4 months, our result being published in MPS 2072409.

2024 CW2 (*n8a5W01*) is an Aten NEA found by LC using our Umbrella suite in KASI images taken during the night 10/11 Feb 2024. The object moved very fast ( $\mu = 9.54''/\text{min}$ ) and appeared as a long trail, being detected by STU (which we include in Figure 6), but it was missed by Tycho (reducer MP) due to lower  $2''/\text{min}$  limit needed to search faster with Tycho. It was estimated at  $R \sim 19.9$  and reported quite promptly as a trailed NEO candidate (15 h after acquisition), being posted on NEOCP and confirmed soon by other stations. Initially it was designated as 2024 CW2, being published in MPEC 2024-C133<sup>44</sup> (credited to our team and KASI W93 station), discovery which vanished soon after it was paired to the older NEA 2007 EG (discovered by Catalina in 2007). Our recovery prolonged its orbit arc from only 6 days to 17 years, being published in MPS 2117530. Thanks to Marco Micheli (ESA) and Miquel Serra-Ricart (Light Bridges and IAC) who recovered this object with their telescopes.

<sup>43</sup><https://www.minorplanetcenter.net/mpec/K24/K24B07.html>

<sup>44</sup><https://minorplanetcenter.net/mpec/K24/K24CD3.html>

Other better known NEAs (having at least two opposition data) were incidentally detected by our survey using ParaSOL and Tycho software. We have checked and reported their positions together with all other known objects, improving their orbits.

#### 4.7.2. Other Related Recoveries

2024 KQ2 (*n5p5410*) is a Phocaea family asteroid recovered by MP with Tycho and later confirmed by our Umbrella suite, observed with the INT. Its appearance was quite bright star-like moving with  $\mu = 1.15''/\text{min}$ , which distinguished as a possible NEA candidate on the  $\epsilon - \mu$  plots, but had a lower NEOR 10%. As it could not be linked to any known object, we reported it 19 h later and recovered it during the next two nights. Later it was designated 2024 KQ2 (MPS 2187290) but it was later paired with the old known object 2014 KL136 (discovered by Pan-STARRS and having an arc of 37 days), actually recovered by our team 10 years later.

2006 JG22 (*W013006*) is another Phocaea recovered by MP with Tycho and later confirmed with STU in a very crowded field observed with the INT. It appeared star-like faint  $R = 22.1$  moving with  $\mu = 1.29''/\text{min}$ , clearly distinguishing in NEAC but having a low NEOR of 13%, so we submitted as a possible NEA candidate. It was later paired to the known 2006 JG22 (discovered by Spacewatch), our recovery being published in MPS 2186529, prolonging the arc from only 28 days to 10 years.

2018 AF77 (*n3o3023*) is a Hungaria asteroid validated by MP with Tycho in co-added KASI images. It looked star-like quite faint  $G = 20.5$ , moving with  $\mu = 1.06''/\text{min}$  which made it a possible NEA candidate of NEAC, with NEOR 24%. It was linked to two previous Pan-STARRS detections (one month before us) and later linked to the known object 2018 AF77 (first seen by Pan-STARRS in 2018), our data (plus the new Pan-STARRS data) becoming second opposition recovery which prolonged its arc from 2 months to 5 years, being published in MPS 2093364 (which updates the 2018 discovery 2n orbit).

2023 TL84 (*n1a9325*) is another Hungaria seen by MP with Tycho in KASI images and later confirmed by the Umbrella suite. It was star-like  $G = 19.7$  moving with  $\mu = 0.79''/\text{min}$  which remained unclear in the  $\epsilon - \mu$  plots but had a high NEOR 72%, being reported as a NEA candidate. It was later paired to the new object 2023 TL84, seen during three nights by Pan-STARRS few days and later linked by an old 2015 1n PS detection, our recovery being published in MPS 2016778.

2021 VC96 (*n1a9327*) is another Hungaria detected by MP with Tycho and later confirmed by ParaSOL in KASI images. It showed as a star-like quite bright  $G = 19.9$  appearance at moderate  $\mu = 0.67''/\text{min}$  whose NEA candidacy remained unclear, being reported among regular unknown asteroids. It was later paired with PS and Catalina observations made before us, then linked to other past detections, then paired with an old 2016 discovery by Catalina. Designated as 2021 VC96, it was actually recovered by our team which prolonged its arc from only 5 days to 7 years (together with other stations), our work being published in MPS 2056765.

2014 BU91 (*n1a9329*) is yet another Hungaria seen by MP with Tycho and later confirmed with ParaSOL in KASI images. It had a star-like trusty detection  $G = 20.3$  and moved with only  $\mu = 0.68''/\text{min}$  which made it unclear NEA candidate, being sent among regular asteroids. It was linked to previous Pan-STARRS 3n detections and later linked to an old 2n arc discovered by Pan-STARRS in 2014, designated 2014 BU91. Our KASI data contributed to the prolongation of its arc from only 12 days to 9 years, being published in MPS 2015685.

2023 XZ27 (*n7a3220*) is a MBA detected in KASI images by MP with Tycho, simultaneously confirmed by STU. Its appearance was star-like and quite bright  $G = 19.8$ , moving with  $\mu = 1.20''/\text{min}$ , which detached on NEAC and had a NEOR of 36%, which we reported as potential NEA candidate. It was later paired with detections of Catalina and Pan-STARRS made during the last month and designed as 2023 XZ27, which was later linked to the old 2017 CS27 (discovered by Catalina), being later probably precovered in older 2016 Subaru data. Our KASI detection (adding those of Pan-STARRS and Catalina) contributed to the second opposition recovery (after 7 years) of this regular MBA object, being published in MPS 2093727.

2022 BE4 (*n8a4100*) is a MC asteroid detected by MP with Tycho in KASI images. Its appearance was star-like, quite faint  $G = 21.6$ , and moving with  $\mu = 1.47''/\text{min}$ , which made it a clear NEA candidate in both models, being submitted quite promptly (13 h after observations). It was later paired by MPC to the old 2022 BE4 object discovered early 2022 by Pan-STARRS. Our work became the only second opposition dataset, prolonging the arc from only 6 days to more than 2 years, being published in MPS 2117312.

#### 4.8. Orbital Improvement of MBAs and Other Known Objects

According to our report count (Tables 2, 4 and 6), during our entire NEA survey we have reported 23,428 known objects (most of them MBAs), which include 3,195 objects observed with the INT, 18,952 with KASI, and 1,281 with T80S. These data were probably published in dozens of MPC publications (MPC, MPS, MPO, MPEC), according to LC and PO.

Three known comets were found in our mini-survey fields (2 using the INT and 1 with KASI). Our data improved their orbits, namely 0049P (published in MPEC 2023-X98), C/2023 S3 (Lemmon) (sent as CK23S030, published in MPEC 2023-X98), and 0150P (MPEC 2024-B57).

#### 4.9. Other Unknown Objects

According to our report count (listed as TOTAL in Tables 2, 4 and 6), during our survey we reported data for 1,374 unknown objects (observed during only 1n), which include 266 INT unknown detections, 1,000 KASI unknown detections and 108 T80S unknown detections, all being stored in the ITF database.

### 5. Comparison between ParaSOL and Tycho

During the first KASI run (3 nights 20230216-18), due to the complexity and amount of KASI data reduction needs, our Umbrella suite was not fully operational, so we preferred to use Tycho based on **IPP** input images to secure slower discoveries in near-real-time. All other nights (KASI, INT and T80S runs), could be reduced with both Tycho and STU, so we can compare the number of detections found by ParaSOL and Tycho.

#### 5.1. Number of Detections and Artifacts

A total of 59 NEA candidates are listed in Tables 3, 5 and 7. In their first column, the candidates found by Tycho but missed by STU appear listed with italic fonts, while those found by STU but missed by Tycho appear underlined.

Four detections (marked as “artifact?” in column *Status*) were found by Tycho with lower confidence, being missed by STU. They should be discarded from comparison, due to artifact risks. Thus, we should compare Tycho with STU using only 55 NEA candidates.

Seven NEA candidates observed with KASI were missed by Tycho during the runs, but were caught by STU (appearing underlined in the NEA candidate Tables). They moved faster ( $\mu = 2.0 - 9.5''/\text{min}$ ), being missed by Tycho due to its  $\mu = 2.0''/\text{min}$  upper proper motion limit used for the large KASI images needed to reduce the runs in near-real-time.

From the 55 NEA candidates to compare, during our surveys Tycho detected 47 candidates, while STU detected 31 candidates (6 INT, 24 KASI and one T80S), meaning 56% STU success fraction from total and 66% comparison STU versus Tycho. This last number is quite similar to the 72% percent mentioned in Section 2.4 found based on an independent KASI dataset, both suggesting the limit of about 70% for the detection capability of the actual version of STU based on the adopted parameter dataset. However, STU outperforms Tycho for fast-moving objects: 7 faster NEAs with apparent motion within the range  $2 - 10''/\text{min}$  being found exclusively by STU.

During the surveys we did not have time to test and tune the STU input parameters in order to improve the number of STU findings without significantly increasing the number of artifacts which were impossible to check and reject by humans during the runs. To report its detections, Tycho calculates an output confidence (classified as High, Medium, Low and None), and during our runs we considered only Tycho detections classified as High and Medium, dropping the others which were extremely numerous (hundreds in each CCD).

Although STU could not be tuned in time to detect higher number of objects compared with Tycho, due to its very fast execution speed (tested below) STU can actually beat Tycho at searching more rapid objects ( $2 < \mu < 10''/\text{min}$  and even faster) in near-real-time (few minutes), and we proved that 7 fastest NEA candidates found by STU were missed by Tycho during the runs due to the need to limit  $\mu$  to  $2''/\text{min}$  to be able to reduce the huge amount of KASI data in near-real-time.

## 5.2. Computing Runtime

We tested the KASI field *n3a2* CCD1 ( $13 \times 60\text{s} \times 85.4$  Gpix images observed at 5/6 Dec 2023) to compare the execution time (only the ST module) of STU (under Linux) versus Tycho (using a few Windows machines), considering two proper motion limits used in our surveys:  $\mu = 2''/\text{min}$  and  $\mu = 10''/\text{min}$ . In this field, Tycho found 101 known objects, while STU found 74 known asteroids, thus 73% of Tycho findings.

Using the Linux *parasol1* machine (CPU AMD Ryzen 9 5950X, RAM 128G, SSD 1T, GPU Radeon RX 6800 XT), we timed STU with about 3 min for  $\mu = 2''/\text{min}$  (15,296 search vectors), and 7 min for  $\mu = 10''/\text{min}$  (365,119 vectors), processing data in both cases with about 1700 Gpix/s.

Using the first Windows machine (CPU Intel(R) Core(TM) i7-14700KF, RAM 64G, GPU NVidia RTX 4090), MP timed Tycho with 2.5 min for  $\mu = 2''/\text{min}$  (10,816 vectors, thus comparable in runtime with STU), and about 3 h for  $\mu = 10''/\text{min}$  (256,036 vectors, thus much slower than STU). Using another Windows machine (*parasol3*: CPU i7 12th 12700k, RAM 64G, SSD 2G, GPU Nvidia RTX 3070Ti), we timed Tycho with 29 min for  $\mu = 2''/\text{min}$  (21,316 search vectors) and about 12 h for  $\mu = 10''/\text{min}$  (515,524 vectors), when setting Tycho at granularity 32% .

We also tested Tycho on two older machines with slower GPUs. First, CB used his Windows PC (CPU AMD Ryzen 3 1200, RAM 8G, GPU NVIDIA GeForce RTX 2070 Super), and timed Tycho with about 31 min for  $\mu = 2''/\text{min}$ , and more than 12 h for  $\mu = 10''/\text{min}$ . Second, OV used his ASUS OMEN laptop (CPU Intel i7-7700HQ, RAM 16G, GPU NVIDIA GeForce GTX 1070), and timed Tycho with 4 h for  $\mu = 2''/\text{min}$  (26,448 vectors), estimating 124 h for  $\mu = 10''/\text{min}$  (649,724 vectors), both run for granularity 50%.

The above Tycho runtimes, specially the extremely large numbers counted on older machines, all obtained for only one KASI CCD (out of 4 CCDs), conclude that Tycho is not feasible to run above  $\mu = 2''/\text{min}$  on any large dataset (more than one Gpix in total for all co-added images), except maybe in a cloud network consisting of many computers (which assume more massive amount of data transfer). Compared with Tycho, albeit yet the smaller number of detections which we hope to improve soon, STU is extremely fast, allowing ST reduction of large datasets (such as KASI) in near-real-time.

The ability of STU to process very large amounts of data in near-real-time during the observing runs is due to a few novel methods implemented since 2021 in Umbrella by the author Malin Stanescu. First, STU introduced a hypothesis rejection design, which allows it to use a very fast brute force scan. Second, STU uses an associative scoring method, which is comparable in computational cost with mean co-addition, while delivering the robustness to outliers of median co-addition. Furthermore, STU uses an order of traversing the search space that improves data locality, allowing the use of cache memory, which has much higher bandwidth. For these reasons, the brute force stage of STU operates at pixel processing rate comparable to the FLOPS rating of the accelerator (the version in this paper achieves  $> 0.5$  pix/lane/clock).

## 6. Pushing the Survey Depth from Blinking to Synthetic Tracking

In this section we compare synthetic tracking versus classic blinking detection, taking into account our experience with automatic blinking algorithms (NEARBY platform) and also visual detection (using Astrometrica), both gathered in the last decade mostly using the INT.

## 6.1. New MagLim EURONEAR Tool

With the aim to measure the limit depth of a survey, recently OV developed a new EURONEAR tool named *MagLim*<sup>45</sup> which plots a histogram counting detections of an input FITS image previously resolved astrometrically, by calculating the photometric zeropoint of the image upon identifying catalog stars based on Gaia DR3 (*RPmag* band) or Pan-STARRS DR1 (Sloan *r* band) catalogs<sup>46</sup>.

The SExtractor detections of *MagLim* are run with the following hard coded parameters: *DETECT\_MINAREA* = 5, *DETECT\_THRESH* = 1.8, *ANALYSIS\_THRESH* = 1.8 (chosen to match the faintest trusted detections, based on very careful visual blink tests), *FILTER* = *Y* and *PHOT\_APERTURES* = 12. In the future, some of these parameters might be changed in the input.

In order to reject noise, only SExtractor detections having *FLAGS* = 0 (only non-contaminated stars or galaxies) are allowed to pass both the zeropoint and counting detection steps. To reject noise (possibly mixed with very faint galaxies), in the counting detection step we propose the default *CLASS\_STAR* = 0.2 value (instead of 0.5 value which ideally separates 50 – 50% stars from galaxies). Moreover, few other parameters are possible to tune in the input: the image seeing (default 1.2", needed to separate stars from galaxies and noise), *CLASS\_STAR*, and the catalog magnitude limit (default 20.0, allowing for the zeropoint calculation to select the most accurate catalog stars for the zeropoint).

The output of *MagLim* is: the number of SExtractor detections, number of catalog stars falling in the field and number of matched detections with catalog stars, the median FWHM of all star-like detections, the image photometric zeropoint (ZP) and the absolute magnitude deviation of the catalog stars used for the ZP calculation, the number of trusted detections used in the histogram, and the histogram plot counting the number of detections plotted in 0.2 mag bins. Based on the histogram, the depth of the field can be simply read out from the highest bin.

*MagLim* could be used to measure photometric depths of either individual images or co-added images processed upon aligning (on stars) and combining (after leveling and using median) of the individual images taken in any ST survey like ParaSOL.

## 6.2. Depth of our Surveys

Based on the *MagLim* tool, we have analyzed the survey depth (assuming ideal stable conditions) and could compare blinking versus synthetic tracking capabilities based on images acquired with the INT, KASI and T80S, by comparing the detection limit of one single image (needed in blinking method) with that of all co-added images (used in the ST method).

In Figure 11 we plot two *MagLim* INT histograms showing the detection limit of one 30 s image (upper panel) compared with the co-add of 12 × 30s images observed with the INT in our field ECL5 CCD4 observed in 18/19 Oct 2023 at airmass ~ 1.6 in dark time and good conditions (image seeing 1.2"). A total of 1506 star-like SExtractor detections could be found in the single INT image (upper panel) with the histogram peak around  $r = 22.0$ , compared with the result obtained upon co-adding 12 × 30 s images (bottom panel) for which *MagLim* found 2106 star-like detections suggesting a detection limit of  $r = 23.2$ , gaining 1.4× more detections and 1.2 mag using ST method compared to blinking. This limit is consistent with the INT WFC SIGNAL exposure time calculator<sup>47</sup> which predicts  $R = 23.0$  limit at SNR 5 for 12 × 30 s images taken in average conditions consistent with our INT runs (gray time, seeing 1.5" and airmass 1.5).

The above limits ( $r = 23.2$  predicted by *MagLim* and  $R = 23.0$  predicted by SIGNAL) are below the limit of  $V \sim 22.5$  predicted by FITSBLINK<sup>48</sup> software for all 3195 known asteroids identified in our entire INT survey, according to the peak shown in the FITSBLINK magnitude-residuals plot. This could be explained by the fact that *MagLim* was run on a field observed in dark time and good seeing (valid for only a small fraction of our INT runs), and

<sup>45</sup><http://www.euronear.org/tools/maglim.php>

<sup>46</sup>Other catalogs, bands and options could be added in the future

<sup>47</sup><http://c.ing.iac.es/signal/signal.php?instrument=WFC>

<sup>48</sup><http://www.fitsblink.net/residuals/>

also by the fact that by running STU we could detect a bit above the known asteroid population run in FITSBLINK, finding other 266 unknown sources, probably fainter than the population of known asteroids.

Similar histograms can be obtained for KASI images, and for the survey field *n3c1* CCD1 (observed during the night 5/6 Dec 2023 at airmass 1.0 in dark and good conditions, seeing 1.1'') we obtained the following result: using only one 60 s image, *MagLim* found 23,264 star-like detections and predicts a depth of  $r = 22.4$ . Using  $12 \times 60$  s images we found a limit of  $r = 24.0$ , while using all 26 images we found 46,913 star-like detections and a limit of  $r = 24.4$ , thus an improvement of  $2.0\times$  and 2.0 mag. The above *MagLim* limit of  $r = 24.0$  for 12 images (used during most of our KASI survey) matches exactly with the FITSBLINK limiting magnitude prediction ( $V \sim 24.0$ ) for 18,952 known asteroids, according to their magnitude dependence of residuals plot.

Taking advantage of the repeated *n3o4* KASI field, we can evaluate the KASI depth reached e.g. in CCD4 (using all 51 available images) observed at 18/19 Feb 2023 at airmass 1.4 in dark time but worse seeing conditions (1.9''). In one image *MagLim* found 10,004 star-like detections, reaching  $r = 21.6$  (lower than the previous KASI field due to worse conditions). In  $12 \times 30$  s co-added images the histogram shows a limit of  $r = 23.0$  (thus 1 mag below the previous set taken in better seeing), while using all 51 co-added images we found 21,784 star-like detections and reach  $r = 23.8$ , thus an increase of  $2.2\times$  and 2.2 magnitudes compared with one single KASI image.

Finally, we studied the similar histogram pair observed with T80S based on the T80S EU12 field (very few density of stars at high galactic latitude) during the night 24/25 Jun 2023 at airmass 1.1 in dark time and average seeing 1.4''. In one image *MagLim* detected 21,538 stars and has reached  $r = 21.8$  limit, while in the whole set  $19 \times 60$ s images it found 34,351 star-like detections and could reach  $r = 22.8$ , thus an increase of  $1.6\times$  and 1.0 magnitude. This limit is consistent with the maximum value of the expected magnitudes ( $V \sim 22.5$ ) predicted by FITSBLINK for all 1281 known asteroids identified in the whole T80S survey, showing in their magnitude-residuals plot.

### 6.3. Probably Missed by Blink

Recently we demonstrated the capability of STU, warning about risk of missing fainter or faster asteroids when using traditional blinking software [53]. Based on some comparison with our NEARBY blink detection pipeline (run in some INT fields), and based on other KASI visual inspection in DS9 blink, here we enumerate some STU or Tycho detections probably missed by any blinking software.

The following 6 trailing objects (all NEAs) were probably lost by other blink software due to fast speed ( $4 < \mu < 10''/\text{min}$ ): *n5b7402* (INT), *n3b1W01*, *n3b3W01*, *n6p5W04*, *n6p3W06* and *n8a5W01* (all KASI).

At least the following 21 NEA candidates (36% of total) were probably lost by traditional blink software due to their faintness (mostly above  $V > 21$ ): *Mar0262*, *N6B6W01*, *n6c2188* (observed with INT); *Mar0414*, *n3o4081*, *n3o4089*, *n3o4097*, *n1b1362*, *n1b1365*, *n1b1367*, *n3a4018*, *n3a5013*, *n3a5015*, *n3b4079*, *n3c1087*, *n3c1088*, *n3c2066*, *n5p5OV1* (observed with KASI, including 2 possible artifacts); and *Mar3087*, *Mar3103*, *Mar3769* (observed with T80S, including 2 possible artifacts).

## 7. NEA Discovery Statistics

Based on a follow-up NEA program using the INT in 2011-2012 in blinking detection mode which covered 24 sq.deg, we predicted about one detectable unknown NEA candidate ( $R < 22.0$ ) to fall in every 2 sq.deg scanned with a 2 m class telescope (mostly in dark time) [62].

Based on our NEA surveys, we can update this statistics, reflecting the actual NEA survey knowledge which has advanced during the last decade, mainly thanks to the U.S. surveys which has grown the number of known NEAs from 9,300 (Oct 2012) to 36,800 (Dec 2024) - a factor of  $4\times$  during the last 12 years.

For these statistics, additionally to the numbers of NEA candidates listed in Tables 2, 4 and 6, we define the *best NEA candidates* as NEA candidates clearly visible (as trails or star-like) in all or most individual images, which move at higher speeds passing both the NEOR and our NEAC criteria (emphasized in bold in the tables). In Tables 3, 5 and

7 we mark in bold (columns 1 and 2) the best 15 NEA candidates, which comprise 4 classes: NEA discoveries, NEA co-discoveries, one-night NEA discoveries, and NEA recoveries (as recorded in the Status column).

Based on our NEA surveys, with the INT we observed mostly in bright and gray time 381 fields covering an area of 103 sq.deg. We found 9 NEA candidates and 4 best NEA candidates (1 discovered, 1 co-discovered and 2 one-night), which makes on average one NEA candidate in about 11 sq.deg and one best NEA candidate in 26 sq.deg, assuming a depth of  $R \sim 23.0$  obtained from  $12 \times 30$  s images.

During our KASI survey, we observed in dark time 142 fields which covered 550 sq.deg, finding 47 NEA candidates and 11 best NEA candidates (4 discovered, 2 co-discovered, 2 one-night and 3 recovered), which make on average one NEA candidate in 12 sq.deg. and one best NEA candidate in 50 sq.deg, assuming a depth of  $R \sim 23.5$  from 12 images and average seeing 1.5".

With the T80S we observed in dark time 13 fields which covered 26 sq.deg, and we found 3 NEA candidates, or one NEA candidate in about 9 sq.deg, assuming a depth of  $R \sim 22.8$  from  $20 \times 60$  s images and average seeing 1.5". No best NEA candidates were found with T80S, due to small number of fields and smaller aperture.

Table 8 summarizes these results. Based on the 3 telescopes, we can draw the conclusion that using ST up to  $R = 23.0 - 23.5$ , on average one NEA candidate can be detected in 9-12 sq.deg (good agreement between all 3 telescopes), while one best NEA candidate can be found in 26-50 sq.deg (quite discrepant result between INT and KASI, possibly due to worse INT conditions and low number statistics). These numbers can be used for planning future similar surveys.

## 8. Conclusions and Future Work

We summarize the conclusions and brief plans for future work.

### 8.1. Conclusions

Based on our past software development work (2015-2019, by MS and OV), other recent experience in blinking detection (2017-2019 in the NEARBY project initiated by OV), and part of the Romanian ParaSOL project (2022-2024, led by PO), we have developed the STU pipeline aimed to detect moving sources (asteroids, NEAs, space debris) in sky surveys, capable to measure astrometry and photometry of all moving sources, flag NEA candidates, and produce MPC reports in near-real-time (during next day). To the best of our knowledge, *our Umbrella software suite* became the first European pipeline for detection of faint moving sources via synthetic tracking.

The *Umbrella* software suite consists of 3 modules, namely the IPP for processing the raw images (by splitting mosaic CCDs, then applying corrections of bias, dark, flat field, re-sampling for optical distortions), STU for the actual detection via synthetic tracking of each reduced CCD, and Webrella for the final human validation of sources.

During the last two years we applied the *Umbrella* software suite to a few mini-surveys of NEAs observed with three survey telescopes:

- The ING's INT 2.5 m diameter, located at ORM in La Palma, endowed with the old 34 Mpix WFC 4-CCD mosaic covering 0.27 sq.deg and *etendue* 1.37. Using the INT we observed in total 100 hours spread in 14 visiting nights (affected by some bad time), plus some service time aimed to recovery, covering in total 104 sq.deg (382 WFC fields), mostly in gray and bright time (only one third dark time), partially affected by some INT tracking problems.
- The Korean KASI 1.6 m diameter, located at CTIO in Chile, endowed with the giant 341 Mpix KMT-Cam 4-CCD mosaic camera covering 4 sq.deg and *etendue* 4.62, Using KASI we observed in total 62 hours spread in 8 service nights plus some service time aimed to recovery, covering 568 sq.deg (142 KASI fields), mostly in dark time.

- The Brazilian T80S 0.8 m diameter, located at CTIO in Chile, endowed with the monolithic 85 Mpix T80Cam-S CCD camera, covering 2 sq.deg and *etendue* 1.0. Using T80S we observed in service mode 7 hours spread in 8 nights, covering 24 sq.deg (12 T80S fields), all in dark time.

During our NEA surveys we obtained the following results, most of them reduced and submitted in near-real-time, generating discoveries or recoveries of NEAs and other orbitally related asteroids, and others generating unfortunate lost objects due to late reduction (mostly few days) or lack of recovery time. During and after each run, we used both our *Umbrella* software suite to detect moving objects in ST mode and also the *Tycho Tracker* software to compare and complete the detection only at slower speeds ( $\mu < 2''/\text{min}$ ). We can summarize here these results:

- We discovered and secured 5 NEAs (credited to our team), from which one was observed with the INT (2023 DZ2, which temporary became a famous VI), and 4 with KASI (2023 XC8, 2023 XV21, 2023 XP14, and 2024 AZ10).
- We co-discovered 3 NEAs (in the same time with Pan-STARRS, sharing the same discovery MPEC, one with INT and 2 with KASI), namely 2024 JJ25, 2023 XA3, 2023 XN12, although our main sky coverage strategy was to avoid overlaps with major surveys.
- We discovered 4 other one-night clear NEAs (fast moving  $\mu > 2.5''/\text{min}$  also visible in blinking mode), nicknamed *n5b7402*, *n6c2188* (observed with INT), *n3b1W01* and *n6p3W06* (KASI), mainly thanks to STU (much faster than Tycho for ST at higher speed), our one-night reports being now stored in the ITF database, possible to p/recover via data mining of the Pan-STARRS, Catalina or maybe other surveys, when such data will become available.
- We discovered other 5 NEA related asteroids, namely 3 Hungarias (2 with INT and another with KASI based on 2n data), plus 2 Mars crossing asteroids (1 with T80S and 2 with KASI), recovering most of them during a lapse of time of 2-3 nights.
- We co-discovered other 5 NEA related asteroids, namely 3 Hungarias (one with the INT and 2 with KASI), one Mars crossing, and another Phocaea (both using KASI), plus at least two more MBAs.
- We found (thus have recovered) 3 poorly known NEAs (previously observed at one opposition, detected all in KASI fields), plus 8 other poorly known related NEA candidates (2 with INT and 6 with KASI), extending their orbital arcs from a few days to up to 17 years.
- We probably discovered up to 21 one-night NEA candidates, most of them probable orbitally related to NEAs (Hungarias, Mars crossing or Phocaea asteroids), all having star-like aspect, including 17 clearly detected with KASI, and 4 possible artifacts (2 with KASI and 2 with T80S), which are stored in the ITF database and could be p/recovered via archival data mining when neighboring observations will become available in external image archives.
- Thanks to our near-real-time reduction, validation, identification and reporting of all moving objects, we improved orbits of 23,428 known mostly MBAs (14% observed with the INT, 81% with KASI, and 5% with T80S), having submitted in total 60,082 positions of known asteroids.
- In all of our surveys, we detected and reported 1374 unknown objects (mostly MBAs, including 19% with the INT, 73% with KASI and 8% with T80S).

To compare classic blinking with synthetic tracking algorithm, under the EURONEAR Tools we developed the public *MagLim* tool which draws a histogram of trusted sources (mostly stars) detected by SExtractor in a FITS input image with previously resolved WCS. Using this new tool, we compared the magnitude limits of individual images versus co-added for all 3 telescopes, finding increases of 1-2 mag and factors of 1.4 – 2 $\times$  increase in number of faint detections. Thus, the main advantage of using ST versus blink (for which only 4-5 images are enough) is the increase of detection of faint objects, and using *MagLim* we proved that one can double the number of detections, with the pitfall of increasing the observed time, namely tripling the time with INT and KASI (2 m class telescopes) or quadrupling it using T80S (1 m class telescope). We enumerated at least 21 faint star-like NEA candidates detected

by STU or Tycho which probably would be missed by other blinking techniques. Another advantage of using ST is the increase of SNR of trailing objects which otherwise miss detection of traditional blinking techniques. We gave examples of 6 trailing objects (clear NEAs) which could be lost by blinking software (ex NEARBY).

Using our surveys taken with 1-2 m class telescopes similar to major US surveys, we evaluated the present NEA discovery statistics using ST techniques which need to spend 3 – 4× more on each field than blinking surveys but could detect fainter and faster NEAs. On average, up to the limit  $R = 23 - 23.5$ , one NEA candidate can be found with ST in every 9-12 sq.deg (quite good agreement of the three telescopes statistics), and one best NEA candidate (a trusted NEA due to its fast speed and visibility in individual images) can be discovered in every 26-50 sq.deg (more discrepant results between INT and KASI, probably due to worse INT observing conditions). These statistics could be important when planning future surveys, based on the actual depth of existing capabilities, left number of NEA populations (based on models), for deciding ST or traditional blinking should be used for best efficiency given a limited amount of observing time.

The computing runtimes of STU and Tycho runs on similar machines suggest similar results between the two software for the detection of slow motion asteroids (below  $2''/\text{min}$ ), but STU becomes much faster than Tycho when searching faster objects (between  $2 - 10''/\text{min}$ ), with Tycho becoming unable to reduce in near-real-time large amounts of survey data (few dozen fields per night) as well as completely incapable to reduce the even larger amount of data that corresponds to very large field of view cameras such as the one of KASI (above 100 Mpix per image).

The biggest advantage of ST (versus blinking) is achieved when using very rapid CMOS cameras (sub-second readout time) instead of slow and mosaic CCD cameras (having readouts of 1-2.5 min such as those installed in the three telescopes used in this survey). The actual CCD readout time can be best used for acquiring more images for ST pipelines, instead of becoming dead time, such as the above instruments which actually wasted half of the awarded time during readouts.

Data derived from our observing runs were included in the following MPC publications:

- 10 MPECs including observations and orbits (new or updated) of NEA candidates (2 from the INT and 8 from KASI).
- 34 MPS's including observations of NEA candidates (7 from the INT, 26 from KASI and one from T80S).
- 3 MPECs including observations and updated orbits of comets falling in our survey fields (2 from INT and one from KASI).
- Probably a few dozen other MPC publications (MPS, MPO, MPC, MPEC) include some of our incidental observations which contributed to orbital improvement of other asteroids (mostly MBAs) reported in our surveys.

## 8.2. Future Work

Further development of our Umbrella suite will depend on available manpower and hopefully on other available funding from Romania or elsewhere. Here we can list just a few directions which could improve our ST capabilities.

- We will reduce with STU our first KASI run (20230216-18), never reduced before due to lack of complete pipeline during our first observing run (reduced with Tycho up to  $\mu = 2''/\text{min}$ ). This could actually generate some fast NEA discoveries (specially if caught during multiple nights in which we observed the same fields) or poorly known NEA recoveries.
- We plan to improve the detection of slower faint star-like sources, by comparison with Tycho (which detects about 20% more such sources than STU, based on the comparison of NEA candidates in this paper) and also based on few older INT archive fields (Stanescu 2025, submitted).
- We need to implement in STU some automatic classification based on some detection confidence (trust score), in order to allow rapid sorting for faster human validation of the many detections automatically found by STU, which can easily leave invalidated the majority of most probably artifacts.

- We plan to test STU for the detection of fastest NEAs or other objects which could skip from one to a neighboring CCD, possible to happen during the entire observing session or for cameras having smaller or/and many CCDs (such as Pan-STARRS 1), objects which otherwise could be missed if CCDs are treated separately. This capability was implemented recently in STU (last version v.0.7 bundle v23-e1) but not tested yet.
- We plan to test STU in cloud environment, and in this sense we acquired four powerful computers funded from ParaSOL project, for which the large amount of KASI data will be useful to test.
- Finally, we hope to test STU for small (< 60 cm) telescopes using CMOS cameras, located in Romania or elsewhere (for better seeing conditions), if any such survey time could become available.

## 9. Acknowledgements

The work of PO, MS, DB, LC, OV and MP was supported by a grant of the *Romanian National Authority for Scientific Research* (UEFISCDI), project number PN-III-P2-2.1-PED-2021-3625 (PI: Marcel Popescu).

The INT observing times was granted from by following Spanish and Dutch TACs: C99 099-MULTIPLE-2/23A, C107 107-MULTIPLE-2/23B, C30 030-MULTIPLE-2/24A (PI: Raul de la Fuente Marcos), and N2 ING.NL.24A.002 (PI: Ovidiu Vaduvescu). The INT is operated on the island of La Palma by the *Isaac Newton Group of Telescopes* in the Spanish *Observatorio del Roque de los Muchachos* of the *Instituto de Astrofísica de Canarias*.

The trip of CB to attend the INT Oct/Nov 2023 observing run was covered by the *University of Craiova*, while FU covered his own trip. CF acknowledges the support from the *Agencia Estatal de Investigacion del Ministerio de Ciencia e Innovacion* (AEI-MCINN) under grant *Hydrated minerals and organic compounds in primitive asteroids* with reference PID2020-120464GB-I00, which allowed her to attend the INT 7-9 May 2024 observing run.

E. Unda-Sanzana acknowledges the observing time awarded by CNTAC to program CN2023A-64 which allowed our KASI and T80S mini-surveys.

This research has made use of the KMTNet system operated by the *Korea Astronomy and Space Science Institute* (KASI) at three host sites of CTIO in Chile, SAAO in South Africa, and SSO in Australia. Data transfer from the host site to KASI was supported by the *Korea Research Environment Open NETwork* (KREONET). Hyori Jeon and JeongHwan Heo supported our KASI observations, while Pujin Kim and SangKyu Yim conducted our KMTNet SAAO service trigger in the attempt to recover our NEA 2023 XP14 discovered with KASI.

We also thank the members of the T80S S-PLUS technical team - funded by the FAPESP grant FAPESP, 2019/26492-3. They took the observations, performed quality checks and quick pre-processing and transferred the raw data to our group in due time. In particular we thank the T80S observers André Luiz Figueiredo, Marcos Antonio Fonseca Faria, André Santos and Luis Angel Gutiérrez Soto. We also acknowledge Fabio Herpich, Marilia Jobim Sartori and Maiara Sampaio for scheduling and logistics, also to Gustavo Bernard Oliveira Schwarz and Eduardo Lacerda for rapid data transfer.

The S-PLUS project, including the T80-South robotic telescope and the S-PLUS scientific survey, was founded as a partnership between the IAG, through Fundação de Amparo à Pesquisa do Estado de São Paulo (FAPESP), the Observatório Nacional (ON, with contributions from the Brazilian funding agencies FINEP, FAPERJ and CNPq), the Federal University of Sergipe (UFS), with important financial and practical contributions from other collaborating institutes in Brazil, Chile (Universidad de La Serena), and Spain (Centro de Estudios de Física del Cosmos de Aragón, CEFCa).

We would like to thank the student collaborator Liviu Stanescu (formerly of the *International Computer High school of Bucharest*, now at *Technische Universiteit Delft*) for helping with the optimization of the KASI crosstalk correction software.

## References

- [1] Akhunzhanov, R.K., Eserkepov, A.V., Tarasevich, Y.Y., 2022. Exact percolation probabilities for a square lattice: site percolation on a plane, cylinder, and torus. *Journal of Physics A: Mathematical and Theoretical* 55, 204004. URL: <http://dx.doi.org/10.1088/1751-8121/ac61b8>, doi:10.1088/1751-8121/ac61b8.
- [2] Allen, R.L., Bernstein, G.M., Malhotra, R., 2002. Observational Limits on a Distant Cold Kuiper Belt. *Astronomical Journal* 124, 2949–2954. doi:10.1086/343773.
- [3] Alvarez, L.W., et al., 1980. Extraterrestrial Cause for the Cretaceous-Tertiary Extinction. *Science* 208, 1095–1108. doi:10.1126/science.208.4448.1095.
- [4] Atwood, B., et al., 2012. Design of the KMTNet large format CCD camera, in: McLean, I.S., Ramsay, S.K., Takami, H. (Eds.), *Ground-based and Airborne Instrumentation for Astronomy IV*, p. 84466G. doi:10.1117/12.925383.
- [5] Bacu, V., 2023. Software solution for detecting asteroids using machine learning techniques, in: *EGU General Assembly Conference Abstracts*, pp. EGU-8676. doi:10.5194/egusphere-egu23-8676.
- [6] Bacu, V., et al., 2019. NEARBY Platform for Detecting Asteroids in Astronomical Images Using Cloud-based Containerized Applications. *arXiv e-prints*, arXiv:1901.04248doi:10.48550/arXiv.1901.04248, arXiv:1901.04248.
- [7] Bacu, V., et al., 2023. Assessment of Asteroid Classification Using Deep Convolutional Neural Networks. *Aerospace* 10, 752. doi:10.3390/aerospace10090752.
- [8] Bernstein, G.M., et al., 2004. The Size Distribution of Trans-Neptunian Bodies. *Astronomical Journal* 128, 1364–1390. doi:10.1086/422919, arXiv:astro-ph/0308467.
- [9] Birlan, M., et al., 2010. More than 160 near Earth asteroids observed in the EURONEAR network. *Astronomy and Astrophysics* 511, A40. doi:10.1051/0004-6361/200912865.
- [10] Borovička, J., et al., 2013. The trajectory, structure and origin of the Chelyabinsk asteroidal impactor. *Nature* 503, 235–237. doi:10.1038/nature12671.
- [11] Howell, E., et al., 1995. The Lowell Observatory Near-Earth-Object Search: A Progress Report, in: *AAS/Division for Planetary Sciences Meeting Abstracts #27*, p. 01.10.
- [12] Buie, M.W., et al., 2024. The New Horizons Extended Mission Target: Arrokoth Search and Discovery. *Planetary Science Journal* 5, 196. doi:10.3847/PSJ/ad676d, arXiv:2403.04927.
- [13] Cegarra Polo, M., et al., 2022. Real-time processing pipeline for automatic streak detection in astronomical images implemented in a multi-GPU system. *Publications of the Astronomical Society of Japan* 74, 777–790. doi:10.1093/pasj/psac035.
- [14] Chiang, E.I., Brown, M.E., 1999. Keck Pencil-Beam Survey for Faint Kuiper Belt Objects. *Astronomical Journal* 118, 1411–1422. doi:10.1086/301005, arXiv:astro-ph/9905292.
- [15] Cochran, A.L., Levison, H.F., Stern, S.A., Duncan, M.J., 1995. The Discovery of Halley-sized Kuiper Belt Objects Using the Hubble Space Telescope. *Astrophysical Journal* 455, 342. doi:10.1086/176581, arXiv:astro-ph/9509100.
- [16] Copandean, D., et al., 2019. Asteroids Detection Technique: Classic “Blink” An Automated Approach. *arXiv e-prints*, arXiv:1901.02542doi:10.48550/arXiv.1901.02542, arXiv:1901.02542.
- [17] Copandean, D., Vaduvescu, O., Gorgan, D., 2019. Automated Prototype for Asteroids Detection. *arXiv e-prints*, arXiv:1901.10469doi:10.48550/arXiv.1901.10469, arXiv:1901.10469.
- [18] Fenucci, M., et al., 2024. The Aegis Orbit Determination and Impact Monitoring System and services of the ESA NEOCC web portal. *arXiv e-prints*, arXiv:2411.03763doi:10.48550/arXiv.2411.03763, arXiv:2411.03763.
- [19] Fraser, W.C., et al., 2008. The Kuiper belt luminosity function from  $m_{\text{SUB}} < 21$  to 26. *Icarus* 195, 827–843. doi:10.1016/j.icarus.2008.01.014, arXiv:0802.2285.
- [20] Fuentes, C.I., et al., 2009. A Subaru Pencil-Beam Search for  $m_R \sim 27$  Trans-Neptunian Bodies. *Astrophysical Journal* 696, 91–95. doi:10.1088/0004-637X/696/1/91, arXiv:0809.4166.
- [21] Gehrels, T. (Ed.), 1992. *Spacewatch discovery of near-Earth asteroids*.
- [22] Gladman, B., et al., 1998. Pencil-Beam Surveys for Faint Trans-Neptunian Objects. *Astronomical Journal* 116, 2042–2054. doi:10.1086/300573, arXiv:astro-ph/9806344.
- [23] Gladman, B., Kavelaars, J.J., 1997. Kuiper Belt searches from the Palomar 5-m telescope. *Astronomy and Astrophysics* 317, L35–L38. doi:10.48550/arXiv.astro-ph/9610150, arXiv:astro-ph/9610150.
- [24] Gladysheva, O., 2020. The Tunguska event. *Icarus* 348, 113837. doi:10.1016/j.icarus.2020.113837.
- [25] Golovich, N., et al., 2021. A New Blind Asteroid Detection Scheme. *arXiv e-prints*, arXiv:2104.03411doi:10.48550/arXiv.2104.03411, arXiv:2104.03411.
- [26] Gorgan, D., et al., 2019. NEARBY Platform for Automatic Asteroids Detection and EURONEAR Surveys, in: *1st NEO and Debris Detection Conference\_ESA2019*, p. 30.
- [27] Heinze, A.N., et al., 2015. Digital Tracking Observations Can Discover Asteroids 10 Times Fainter Than Conventional Searches. *Astronomical Journal* 150, 125. doi:10.1088/0004-6256/150/4/125, arXiv:1508.01599.
- [28] Hodapp, K.W., et al., 2004. Design of the Pan-STARRS telescopes. *Astronomische Nachrichten* 325, 636–642. doi:10.1002/asna.200410300.
- [29] Holman, M.J., et al., 2004. Discovery of five irregular moons of Neptune. *Nature* 430, 865–867. doi:10.1038/nature02832.
- [30] Ishida, K., Mikami, T., Kosai, H., 1984. Size distribution of asteroids. *Publications of the Astronomical Society of Japan* 36, 357–370.
- [31] Kavelaars, J.J., et al., 2004. The discovery of faint irregular satellites of Uranus. *Icarus* 169, 474–481. doi:10.1016/j.icarus.2004.01.009.
- [32] Kim, S.L., et al., 2016a. Crosstalk Correction of the KMTNet Mosaic CCD Image. *Publication of Korean Astronomical Society* 31, 35–41. doi:10.5303/PKAS.2016.31.3.035.

- [33] Kim, S.L., et al., 2016b. KMTNET: A Network of 1.6 m Wide-Field Optical Telescopes Installed at Three Southern Observatories. *Journal of Korean Astronomical Society* 49, 37–44. doi:10.5303/JKAS.2016.49.1.37.
- [34] Koschny, D., Busch, M., 2015. The Teide Observatory Tenerife Asteroid Survey. *Planetary and Space Science* 118, 305–310. doi:10.1016/j.pss.2015.08.007.
- [35] Larson, S., et al., 2003. The CSS and SSS NEO surveys, in: AAS/Division for Planetary Sciences Meeting Abstracts #35, p. 36.04.
- [36] Lee, C.U., et al., 2014. Observational performance of the KMTNet, in: Stepp, L.M., Gilmozzi, R., Hall, H.J. (Eds.), *Ground-based and Airborne Telescopes V*, p. 91453T. doi:10.1117/12.2055571.
- [37] Mainzer, A., et al., 2011. Preliminary Results from NEOWISE: An Enhancement to the Wide-field Infrared Survey Explorer for Solar System Science. *Astrophysical Journal* 731, 53. doi:10.1088/0004-637X/731/1/53, arXiv:1102.1996.
- [38] McMillan, R.S., Spacewatch Team, 2006. Spacewatch Preparations for the Era of Deep All-Sky Surveys, in: AAS/Division for Planetary Sciences Meeting Abstracts #38, p. 58.07.
- [39] Mendes de Oliveira, C., et al., 2019. The Southern Photometric Local Universe Survey (S-PLUS): improved SEDs, morphologies, and redshifts with 12 optical filters. *Monthly Notices of the Royal Astronomical Society* 489, 241–267. doi:10.1093/mnras/stz1985, arXiv:1907.01567.
- [40] Parrott, D., 2020. Tycho Tracker: A New Tool to Facilitate the Discovery and Recovery of Asteroids Using Synthetic Tracking and Modern GPU Hardware, in: Buchheim, R.K., Gill, R.M., Green, W., Martin, J.C., Stephens, R. (Eds.), *39th Annual Conference of the Society for Astronomical Sciences (SAS-2020)*, pp. 101–110.
- [41] Popescu, M.M., et al., 2023. Discovery and physical characterization as the first response to a potential asteroid collision: The case of 2023 DZ<sub>2</sub>. *Astronomy and Astrophysics* 676, A126. doi:10.1051/0004-6361/202346751, arXiv:2306.11347.
- [42] Pravdo, S.H., et al., 1999. The Near-Earth Asteroid Tracking (NEAT) Program: an Automated System for Telescope Control, Wide-Field Imaging, and Object Detection. *Astronomical Journal* 117, 1616–1633. doi:10.1086/300769.
- [43] Reddy, V., et al., 2024. 2023 DZ2 Planetary Defense Campaign. *The Planetary Science Journal* 5, 141. doi:10.3847/PSJ/ad4a6d.
- [44] Sako, S., et al., 2018. The Tomo-e Gozen wide field CMOS camera for the Kiso Schmidt telescope, in: Evans, C.J., Simard, L., Takami, H. (Eds.), *Ground-based and Airborne Instrumentation for Astronomy VII*, p. 107020J. doi:10.1117/12.2310049.
- [45] Schirmer, M., 2013. THELI: Convenient Reduction of Optical, Near-infrared, and Mid-infrared Imaging Data. *The Astrophysical Journal Supplement* 209, 21. doi:10.1088/0067-0049/209/2/21, arXiv:1308.4989.
- [46] Schmithuesen, O., et al., 2007. THELI – A Wide-Field-Imaging Data Processing Pipeline. *Astronomische Nachrichten* 328, 701.
- [47] Shao, M., et al., 2014. Finding Very Small Near-Earth Asteroids using Synthetic Tracking. *Astrophysical Journal* 782, 1. doi:10.1088/0004-637X/782/1/1, arXiv:1309.3248.
- [48] Shao, M., et al., 2017. A constellation of SmallSats with synthetic tracking cameras to search for 90% of potentially hazardous near-Earth objects. *Astronomy and Astrophysics* 603, A126. doi:10.1051/0004-6361/201629809, arXiv:1503.07944.
- [49] Stefanut, T., et al., 2019a. NEARBY Platform: Algorithm for Automated Asteroids Detection in Astronomical Images. arXiv e-prints, arXiv:1901.02545doi:10.48550/arXiv.1901.02545, arXiv:1901.02545.
- [50] Stefanut, T., et al., V., 2019b. Automated Near Earth Asteroids discovery from Astronomical Images using the NEARBY Platform, in: EGU General Assembly Conference Abstracts, p. 16934.
- [51] Stokes, G.H., et al., 2000. Lincoln Near-Earth Asteroid Program (LINEAR). *Icarus* 148, 21–28. doi:10.1006/icar.2000.6493.
- [52] Stănescu, M., Văduvescu, O., 2021. The Umbrella software suite for automated asteroid detection. *Astronomy and Computing* 35, 100453. doi:10.1016/j.ascom.2021.100453, arXiv:2008.04724.
- [53] Stănescu, M.O., et al., 2023. Blink and You Miss It: Real-Time Synthetic Tracking for Near-Earth Object Surveys, in: *Asteroids, Comets, Meteors Conference*, p. 2361.
- [54] Tody, D., 1986. The IRAF Data Reduction and Analysis System, in: Crawford, D.L. (Ed.), *Instrumentation in astronomy VI*, p. 733. doi:10.1117/12.968154.
- [55] Tody, D., 1993. IRAF in the Nineties, in: Hanisch, R.J., Brissenden, R.J.V., Barnes, J. (Eds.), *Astronomical Data Analysis Software and Systems II*, p. 173.
- [56] Tonry, J.L., et al., 2018. ATLAS: A High-cadence All-sky Survey System. *Publications of the Astronomical Society of the Pacific* 130, 064505. doi:10.1088/1538-3873/aabadf, arXiv:1802.00879.
- [57] Urechiatu, R., et al., 2023. Ensemble Machine Learning Model for Automated Asteroid Detection. *Romanian Astronomical Journal* 33, 111–125.
- [58] Văduvescu, O., et al., 2008. EURONEAR: First results. *Planetary and Space Science* 56, 1913–1918. doi:10.1016/j.pss.2008.02.025.
- [59] Văduvescu, O., et al., 2009. EURONEAR: Data mining of asteroids and Near Earth Asteroids. *Astronomische Nachrichten* 330, 698. doi:10.1002/asna.200811198, arXiv:0906.5030.
- [60] Văduvescu, O., et al., 2011a. EURONEAR—Recovery, follow-up and discovery of NEAs and MBAs using large field 1-2 m telescopes. *Planetary and Space Science* 59, 1632–1646. doi:10.1016/j.pss.2011.07.014, arXiv:1108.5780.
- [61] Văduvescu, O., et al., 2011b. Mining the CFHT Legacy Survey for known Near Earth Asteroids. *Astronomische Nachrichten* 332, 580–589. doi:10.1002/asna.201011550, arXiv:1107.2249.
- [62] Văduvescu, O., et al., 2013a. 739 observed NEAs and new 2-4 m survey statistics within the EURONEAR network. *Planetary and Space Science* 85, 299–311. doi:10.1016/j.pss.2013.06.026, arXiv:1308.5594.
- [63] Văduvescu, O., et al., 2013b. Mining the ESO WFI and INT WFC archives for known Near Earth Asteroids. Mega-Precovery software. *Astronomische Nachrichten* 334, 718–728. doi:10.1002/asna.201211720, arXiv:1301.6902.
- [64] Văduvescu, O., et al., 2015. First EURONEAR NEA discoveries from La Palma using the INT. *Monthly Notices of the Royal Astronomical Society* 449, 1614–1624. doi:10.1093/mnras/stv266.
- [65] Văduvescu, O., et al., 2017. Data mining of near-Earth asteroids in the Subaru Suprime-Cam archive. *Astronomische Nachrichten* 338, 527–535. doi:10.1002/asna.201713296, arXiv:1704.03936.

- [66] Vaduvescu, O., et al., 2018. 280 one-opposition near-Earth asteroids recovered by the EURONEAR with the Isaac Newton Telescope. *Astronomy and Astrophysics* 609, A105. doi:10.1051/0004-6361/201731844, arXiv:1711.00709.
- [67] Vaduvescu, O., et al., 2020. Dozens of virtual impactor orbits eliminated by the EURONEAR VIMP DECam data mining project. *Astronomy and Astrophysics* 642, A35. doi:10.1051/0004-6361/202038666, arXiv:2009.00807.
- [68] Vaduvescu, O., et al., 2021. Ready for EURONEAR NEA surveys using the NEARBY moving source detection platform. *New Astronomy* 88, 101600. doi:10.1016/j.newast.2021.101600.
- [69] Whidden, P.J., et al., 2019. Fast Algorithms for Slow Moving Asteroids: Constraints on the Distribution of Kuiper Belt Objects. *Astronomical Journal* 157, 119. doi:10.3847/1538-3881/aafd2d, arXiv:1901.02492.
- [70] Wright, E.L., et al., 2010. The Wide-field Infrared Survey Explorer (WISE): Mission Description and Initial On-orbit Performance. *Astronomical Journal* 140, 1868–1881. doi:10.1088/0004-6256/140/6/1868, arXiv:1008.0031.
- [71] Yanagisawa, T., et al., 2005. Automatic Detection Algorithm for Small Moving Objects. *Publications of the Astronomical Society of Japan* 57, 399–408. doi:10.1093/pasj/57.2.399.
- [72] Yanagisawa, T., et al., 2021. New NEO Detection Techniques using the FPGA. *Publications of the Astronomical Society of Japan* 73, 519–529. doi:10.1093/pasj/psab017.
- [73] Yoshida, F., et al., 2024. A deep analysis for New Horizons' KBO search images. *Publications of the Astronomical Society of Japan* 76, 720–732. doi:10.1093/pasj/psae043, arXiv:2407.05673.
- [74] Zhai, C., et al., 2014. Detection of a Faint Fast-moving Near-Earth Asteroid Using the Synthetic Tracking Technique. *Astrophysical Journal* 792, 60. doi:10.1088/0004-637X/792/1/60, arXiv:1403.4353.
- [75] Zhai, C., et al., 2020. Synthetic Tracking Using ZTF Deep Drilling Data Sets. *Publications of the Astronomical Society of the Pacific* 132, 064502. doi:10.1088/1538-3873/ab828b, arXiv:1907.11299.
- [76] Zhai, C., et al., 2024. Near-Earth Object Observations using Synthetic Tracking. *Publications of the Astronomical Society of the Pacific* 136, 034401. doi:10.1088/1538-3873/ad23fc, arXiv:2401.03255.

Telescope	Site	Diam (m)	F/D	Camera	CCDs Pixels	Scale ('')	FOV ('x')	Etendue (m <sup>2</sup> sq.deg)	MPC
INT	ORM	2.54	F/3.3	WFC	4 4100x2048	0.33	34x34	1.37	950
KASI	CTIO	1.60	F/3.0	KMTS	4 9232x9232	0.40	123x123	8.03	807
T80S	CTIO	0.83	F/4.3	T80Cam-S	9236x9216	0.55	85x85	1.06	807,W93

**Table 1**

The characteristics of the telescopes used for our NEA mini-surveys observed during our ParaSOL project.

Date	Nr.fields	Obs.Time	Known	Unknown	NEA cand
<b>20230227</b>	24	7	428	73	1
<b>20230228</b>	25	8	434	43	0
<b>20230301</b>	29	9	291	16	1
20230302	8	3	99	2	0
20230303	3	1	13	1	0
<b>20230410</b>	28	8	60	0	0
<b>20230411</b>	8	3	9	0	0
20231018	8	2	146	2	0
<b>20231029</b>	12	2	47	1	0
<b>20231031</b>	12	4	30	2	0
<b>20231101</b>	21	10	177	9	0
<b>20231102</b>	30	10	218	35	1
20231103	1	0.5	0	1	0
20231104	1	0.5	0	1	0
<b>20240509</b>	27	6	5	0	0
<b>20240528</b>	33	6	352	27	1
<b>20240529</b>	33	6	322	20	2
<b>20240530</b>	34	6	243	19	2
<b>20240531</b>	36	6	256	7	1
20240601	2	0.5	14	0	0
20240602	2	0.5	18	0	0
20240603	4	1	33	7	0
<b>TOTAL</b>	<b>381</b>	<b>100</b>	<b>3195</b>	<b>266</b>	<b>9</b>

**Table 2**

The INT observing log comprising of 14 visiting nights and some service time for recoveries.

Nickname	Desig	Orbit	Obs.Night	Field	CCD	Img	Exp	Appearance	Mag	PA	$\mu$	$\epsilon$	NEAC	NEOR	Red	n	Status	Publications
<b>E309252</b>	2023 DZ2	Apollo	20230227	n101	3	12	45	star-like	G 20.1	276.4	0.72	140.5	clear	100	CB	3	NEA disc	1810607,2023-F12
<i>Mar0262</i>	2023 BE16	Hungaria	20230301	n367	3	12	45	star-like	G 21.0	226.5	0.73	145.7	clear	11	MP	1	co-disc	1916342
KA01044	2023 VG4	Hungaria	20231102	C9RR1F2	1	8	45	star-like	G 20.9	278.9	0.90	153.3	detached	46	PO	3	disc	2034097
<b>n4b3169</b>	2024 JJ25	Apollo	20240528	n4b3	1	9	30	star like	G 19.3	319.6	1.05	202.0	clear	93	MP	2	NEA co-disc	21793354,2024-K132
<b>n5b7402</b>	2024 KQ2	Phocaea	20240529	n5b7	4	9	30	small trail	G 20.8	315.8	7.09	191.9	clear	100	OV	1	NEA lost	ITF
n5p5410	2024 KL8	Hungaria	...	n5p5	4	9	30	star-like	G 19.8	230.9	1.15	182.4	clear	10	MP	3	10y-rec	2187290
N6B6W01	2024 KL8	Hungaria	20240530	n6b6	1	9	30	star-like	R 22.2	334.3	1.07	195.0	clear	10	MS	3	disc	2201381
<b>n6c2188</b>	...	...	...	n6c2	1	9	30	faint	G 20.2	336.1	2.50	182.8	clear	97	OV	1	NEA lost	ITF
W013006	2006 JG22	Phocaea	20240531	n7r2	2	9	30	faint	R 22.1	229.6	1.29	186.0	clear	13	PO	1	18y-rec	2186529

Table 3: Features of the 9 NEA candidates detected during the INT mini-surveys.

Date	Nr.fields	Obs.Time	Known	Unknown	NEA cand
<b>20230216</b>	15	7	3871	153	0
<b>20230217</b>	15	8	2677	57	2
<b>20230218</b>	20	9	4751	45	4
<b>20231022</b>	15	6	510	14	14
<b>20231023</b>	8	4	513	4	0
<b>20231205</b>	15	7	2181	178	14
20231207	2	1	50	49	1
20231208	5	2	22	21	3
20231210	7	4	57	53	3
<b>20240111</b>	19	7	1596	191	4
<b>20240210</b>	21	7	2724	235	2
TOTAL	142	62	18952	1000	47

**Table 4**

The KASI observing log comprising of 8 service nights and some DDT time for recoveries.

Nickname	Design	Orbit	Obs.Night	Field	CCD	Img	Exp	Appearance	Mag	PA	$\mu$	$\epsilon$	NEAC	NEOR	Red	n	Status	Publications
Mar0414	2021 JD70	Hungaria	20230217	n2o1	1	9	60	star-like	G 20.7	326.5	1.03	160.4	clear	19	MP	3	co-disc	1747047,1973576
Mar0484	2019 RE	MC	...	...	3	9	60	star-like	G 20.9	244.0	1.07	161.4	clear	14	MP	2	follow-up	1747023,1973066
Mar0817	2022 XP8	MC	...	n2o3	3	9	60	star-like	G 21.7	328.6	1.07	161.0	clear	12	MP	2	co-disc	2056838
n3o3023	2018 AF77	Hungaria	20230218	n3o3	3	8	60	star-like	G 20.5	246.8	1.06	161.3	clear	24	MP	1	rec	2093364
n3o4081	...	...	...	n3o4	3	51	60	star-like	G 20.3	336.3	1.30	161.6	clear	36	MP	1	lost	ITF
n3o4089	...	...	...	...	4	51	60	faint	G 20.7	244.1	0.80	160.0	clear	10	MP	1	artifact?	ITF
n3o4097	...	...	...	...	4	51	60	limit	G 20.8	244.2	0.99	160.4	clear	16	MP	1	lost	ITF
nLe8new	...	...	20231022	n1e8	3	8	60	star-like	G 20.6	91.6	0.31	272.1	unclear	69	OV	1	lost	ITF
n1a4704	2023 RE156	MBA	...	n1a4	2	12	60	star-like	G 20.4	324.5	1.12	227.2	detached	36	MP	1	co-disc	2117400
n1a9325	2023 TL84	Hungaria	...	n1a9	2	13	60	star-like	G 19.7	215.9	0.79	135.8	unclear	72	MP	2	3d-rec	2016778
n1a9326	...	...	...	...	3	13	60	star-like	G 20.7	235.3	0.68	135.1	unclear	62	MP	1	lost	ITF
n1a9327	2021 VC96	Hungaria	...	...	4	13	60	star-like	G 19.9	257.1	0.67	134.5	unclear	62	MP	1	7y-rec	2056765
n1a9328	2023 TAI74	Phocaea	...	...	4	13	60	star-like	G 20.2	286.2	0.70	134.6	unclear	22	MP	2	co-disc	2093639
n1a9329	2014 BU91	Hungaria	...	...	4	13	60	star-like	G 20.3	224.3	0.68	134.9	unclear	29	MP	1	9y-rec	2015685
n1b1361	2023 TG143	MBA	...	n1b1	1	25	60	star-like	G 20.4	249.6	0.55	132.4	unclear	34	MP	1	co-disc	2057007
n1b1362	...	...	...	...	1	25	60	fuzzy	G 21.2	218.6	0.73	133.3	unclear	56	MP	1	lost	ITF
n1b1363	...	...	...	...	1	25	60	star-like	G 21.0	228.4	0.61	132.1	unclear	35	MP	1	lost	ITF
n1b1364	...	...	...	...	1	25	60	fuzzy	G 20.5	221.2	0.67	132.7	unclear	39	MP	1	lost	ITF
n1b1365	...	...	...	...	1	25	60	faint	G 20.7	203.7	0.81	133.1	unclear	53	MP	1	lost	ITF
n1b1366	2023 TH198	Hungaria	...	...	2	25	60	star-like	G 23.5	257.7	0.62	132.9	unclear	11	MP	1	co-disc	2254292
n1b1367	...	...	...	...	2	25	60	faint	G 20.7	186.4	1.18	132.9	detached	74	MP	1	lost	ITF
n3a4018	...	...	20231205	n3a4	2	12	60	limit	G 20.2	346.1	0.90	109.4	detached	95	MP	1	artifact?	ITF
n3a5013	2020 UG73	MBA	...	n3a5	3	13	60	star-like	G 19.5	66.0	0.58	114.0	unclear	70	MP	1	follow-up	2056660
n3a5015	2023 UE5	MC	...	...	3	13	60	star-like	G 21.0	46.0	1.47	114.6	clear	98	MP	1	follow-up	2055449
n3b1W01	...	...	...	n3b1	1	13	60	small trail	~20	301.7	5.48	150.2	clear	100	OV	1	NEA lost	ITF
n3b3W01	2023 XA3	Apollo	...	n3b3	2	13	60	long trail	G 21.2	112.8	7.82	152.7	clear	100	PO	1	NEA co-disc	2057153,2023-X123
n3b3W02	2023 XC8	Amor	...	...	2	13	60	small trail	G 21.1	99.4	2.51	153.4	clear	100	PO	3	NEA disc	2072562,2023-X212
n3b4079	...	Hungaria?	...	n3b4	1	12	60	faint	G 20.4	294.6	0.98	151.2	detached	84	MP	2	not linked	ITF
n3c1087	...	...	...	n3c1	1	26	60	faint	G 21.7	0.6	1.07	131.0	detached	97	MP	1	lost	ITF
n3c1088	...	...	...	...	1	26	60	star-like	G 20.6	247.5	0.63	130.8	unclear	57	MP	1	lost	ITF
n3c1089	...	...	...	...	1	26	60	star-like	G 21.2	281.3	0.70	131.5	unclear	65	MP	1	lost	ITF
n3c1092	...	...	...	...	2	26	60	faint	G 22.4	227.3	1.61	131.2	detached	100	MP	1	lost	ITF
n3c1093	2023 XV21	Apollo	...	...	2	26	60	star-like	G 20.8	196.1	1.63	131.9	detached	93	MP	3	NEA disc	2079759,2024-A06
n3c2066	2021 PF10	Amor	...	n3c2	2	24	60	faint	G 22.5	288.6	0.83	129.3	detached	92	MP	1	NEA 2y-rec	2093525,2024-B07
n3c2067	...	...	...	...	4	24	60	star-like	G 22.4	233.3	0.77	128.3	detached	64	MP	1	lost	ITF
n5p1107	2023 XB44	MC	20231208	n5p1	3	13	60	faint	G 21.2	239.2	0.91	151.8	clear	49	MP	1	lost	ITF
n5p3001	2023 QS3	Amor	...	n5p3	4	12	60	star-like	G 21.0	350.2	2.31	131.6	clear	99	OV	1	NEA 4m-rec	2267050
n5p5OV1	...	...	...	n5p5	4	12	60	star-like	G 21.0	350.2	2.31	131.6	clear	99	OV	1	NEA 4m-rec	2267050
n6p2018	2023 XN12	Apollo	20231210	n6p2	2	13	60	faint	G 21.5	299.6	2.11	153.5	clear	100	MP	1	NEA co-disc	2072573,2023-X270
n6p5W04	2023 XP14	Apollo	...	n6p5	4	15	60	small trail	~20	167.3	4.65	133.0	clear	100	LC	1	NEA disc	2072578,2023-X310
n6p3W06	...	...	...	n6p3	2	20	60	small trail	G 21.5	179.8	4.06	130.2	clear	100	LC	1	NEA lost	ITF
n7a1206	...	...	20240111	n7a1	2	10	60	star-like	G 20.3	344.5	1.36	140.1	detached	45	MP	1	lost	ITF
n7a2416	...	...	...	n7a2	4	10	60	faint	G 20.7	329.0	1.12	141.1	detached	29	MP	1	lost	ITF
2023 XZ27	...	MBA	...	n7a3	2	10	60	star-like	G 19.8	340.5	1.20	143.5	detached	36	MP	1	7y-rec	2093727
2024 AZ10	...	Apollo	...	n7b3	2	10	60	faint	G 21.9	351.9	0.49	141.1	unclear	12	MP	1	NEA disc	2117466,2024-C39
2022 BE4	...	MC	20240210	n8a4	1	10	60	star-like	G 21.6	357.0	1.47	115.5	clear	95	MP	1	2y-rec	2117312
2024 CW2	...	Aten	...	n8a5	2	10	60	long trail	R 19.9	346.7	9.54	121.6	clear	100	LC	1	NEA 17y-rec	2117530,2024-C133

Table 5: Features of the 47 NEA candidates detected during the KASI mini-surveys.

Date	Nr.fields	Obs.Time	Known	Unknown	NEA cand
20230523	3	1.5	166	20	2
20230524	2	1.0	240	24	0
20230526	1	0.5	93	8	0
20230607	2	1.0	224	1	0
20230610	1	0.5	111	9	0
20230615	2	1.0	177	29	1
20230624	2	1.0	270	17	0
TOTAL	13	6.5	1281	108	3

**Table 6**

The T80S observing log comprising of 7 partial service nights.

Nickname	Desig	Orbit	Obs.Night	Field	CCD	Img	Exp	Appearance	Mag	PA	$\mu$	$\epsilon$	NEAC	NEOR	Red	n	Status	Publications
<i>Mar3087</i>			20230523	EU05	1	20	60	limit	G 20.2	102.6	1.95	228.7	clear	99	MP	1	artifact?	ITF
<i>Mar3103</i>			...	...	1	20	60	limit	G 20.5	304.1	1.82	229.6	clear	100	MP	1	artifact?	ITF
<i>Mar3769</i>	2023 MD1	MC	20230615	EU11	1	20	60	star-like	G 20.4	135.1	0.76	225.7	detached	90	MP	1	disc	1894649

Table 7: Features of the 3 NEA candidates detected during the T80S mini-surveys.

Telescope	Coverage (sq.deg)	Depth ( $R$ )	NEA candidates		Best NEA candidates	
			Number	Density (1/sq.deg)	Number	Density (1/sq.deg)
INT	103	23.0	9	12	4	26
KASI	550	23.5	47	12	11	50
T80S	26	22.8	3	9	0	—

**Table 8**

The ParaSOL NEA surveys statistics for the three telescopes.

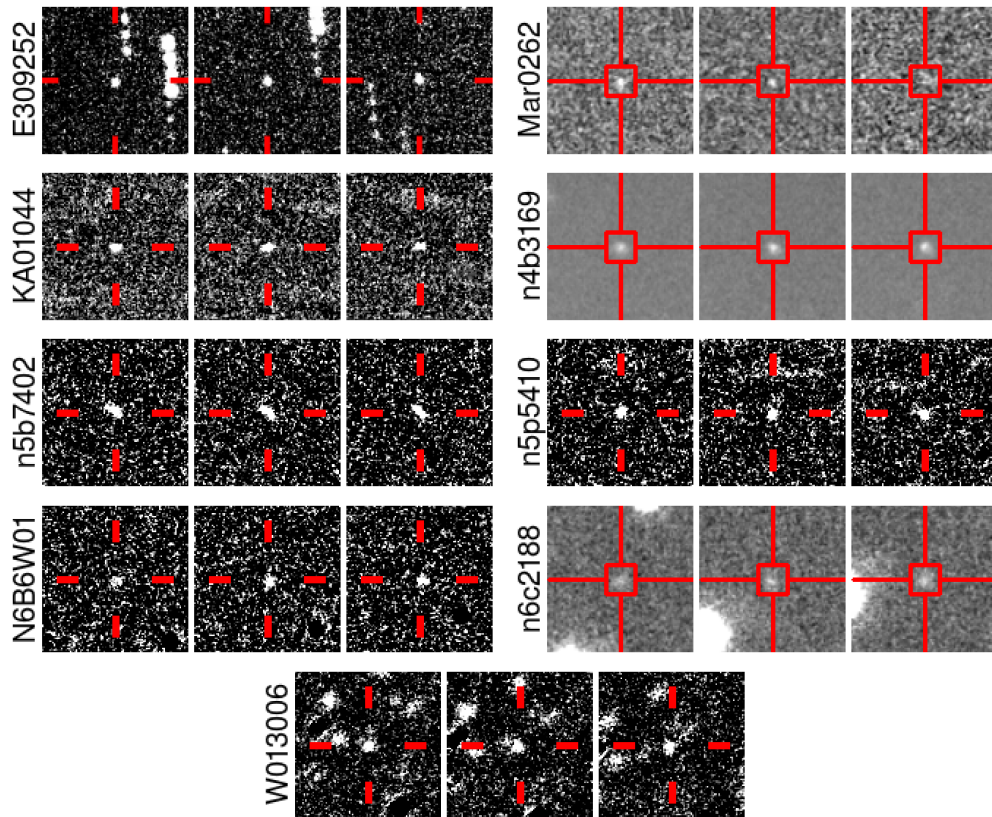
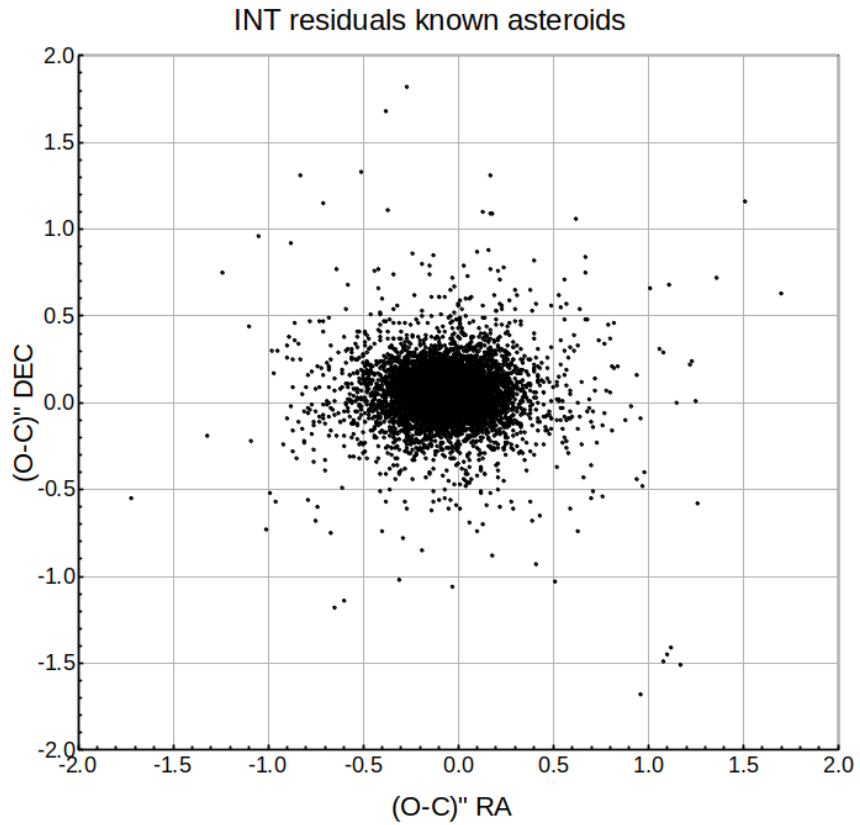
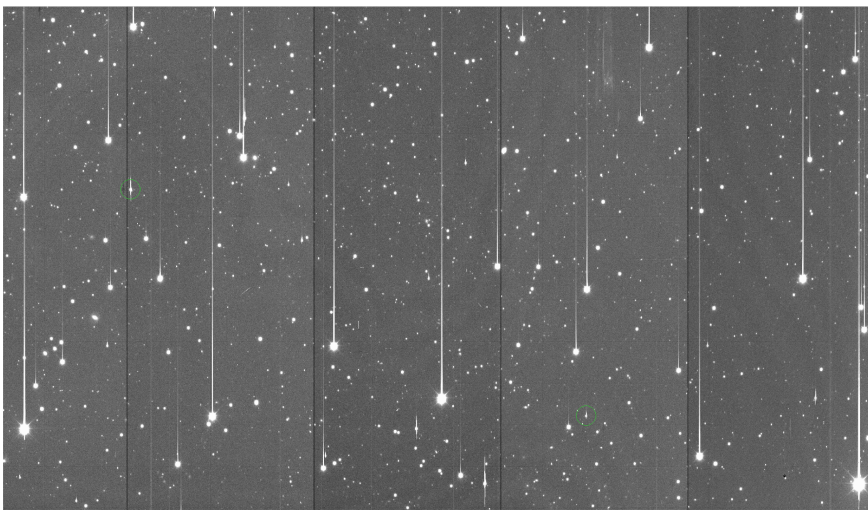


Figure 1: INT NEA candidates detections.



**Figure 2:** The residuals of known asteroids found in the entire INT mini-survey.



**Figure 3:** Online animated GIF presenting the KASI correction of the cross-talk effect, which fixes hundreds of artifact residuals generated by bright stars located in neighboring CCDs or stripes (few brighter ones marked with green circles).



**Figure 4:** Online animated GIF demonstrating the KASI bleeding correction which fixes most of hundreds of columns residuals of bright stars due to reading process.

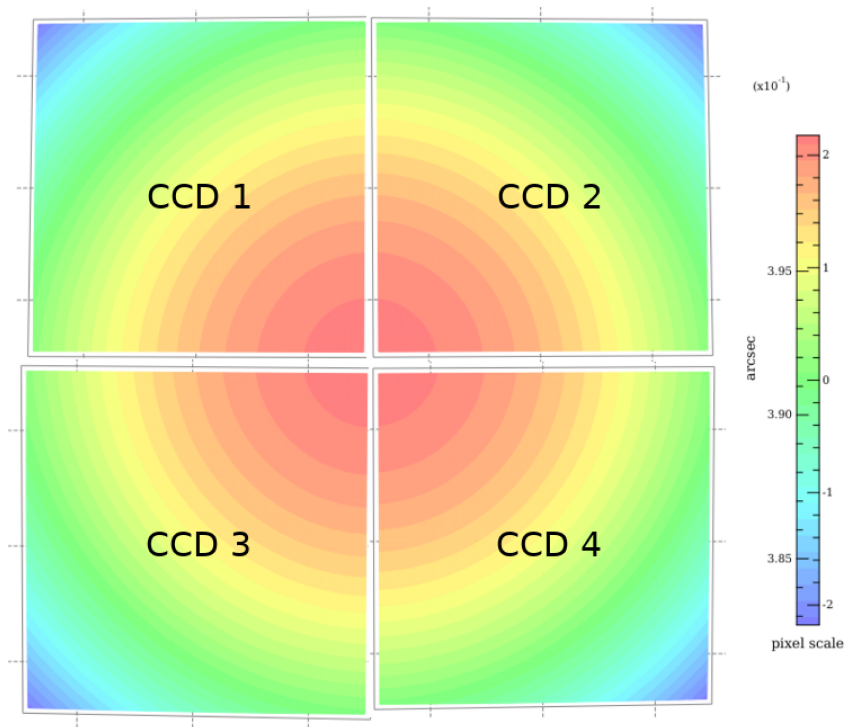


**Figure 5:** Typical KASI Scamp distortion plot displayed as a mosaic created manually from the 4 Scamp CCD individual plots.

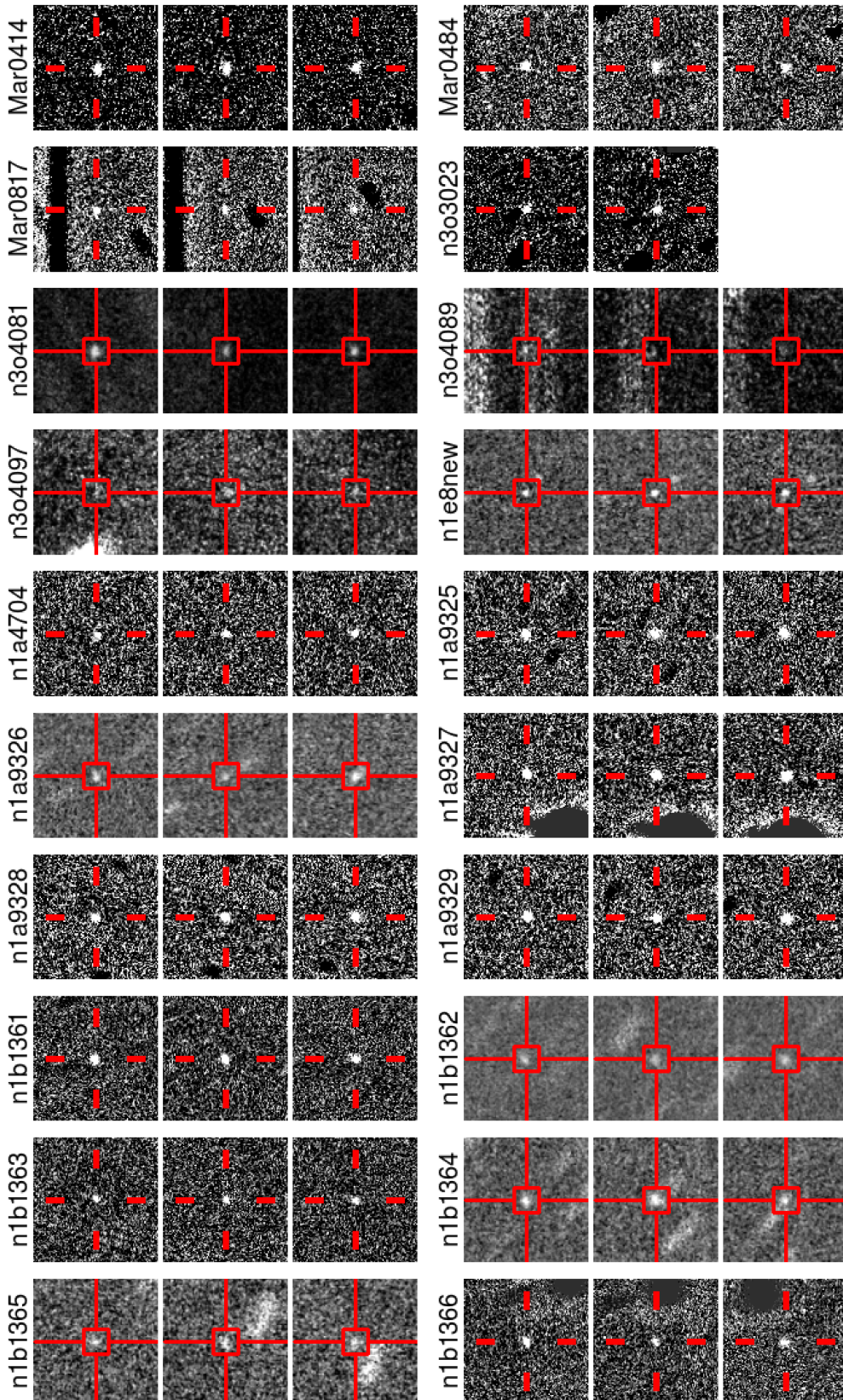


Figure 6: KASI NEA candidates detections.

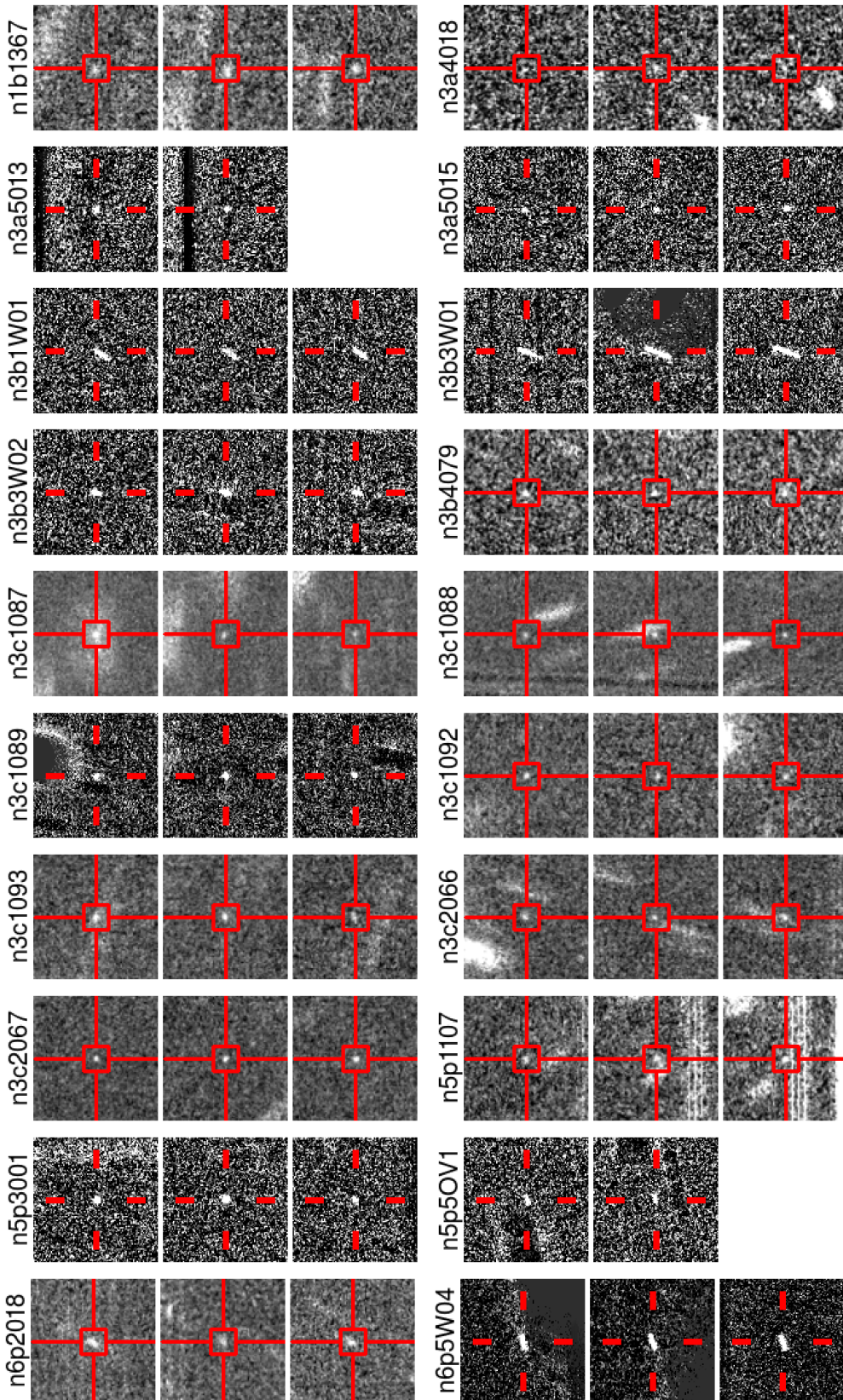
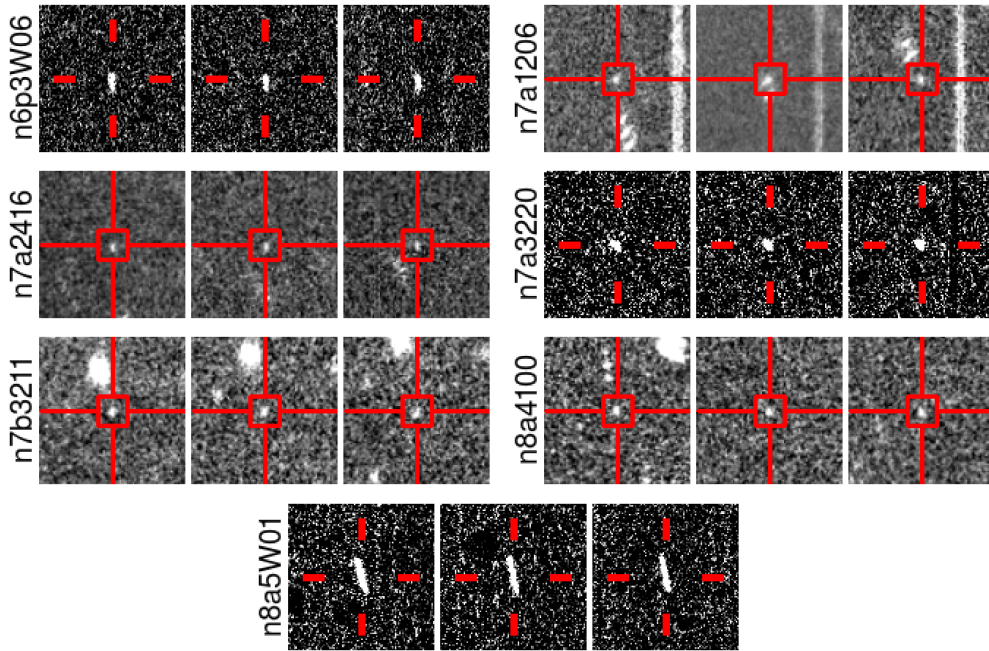
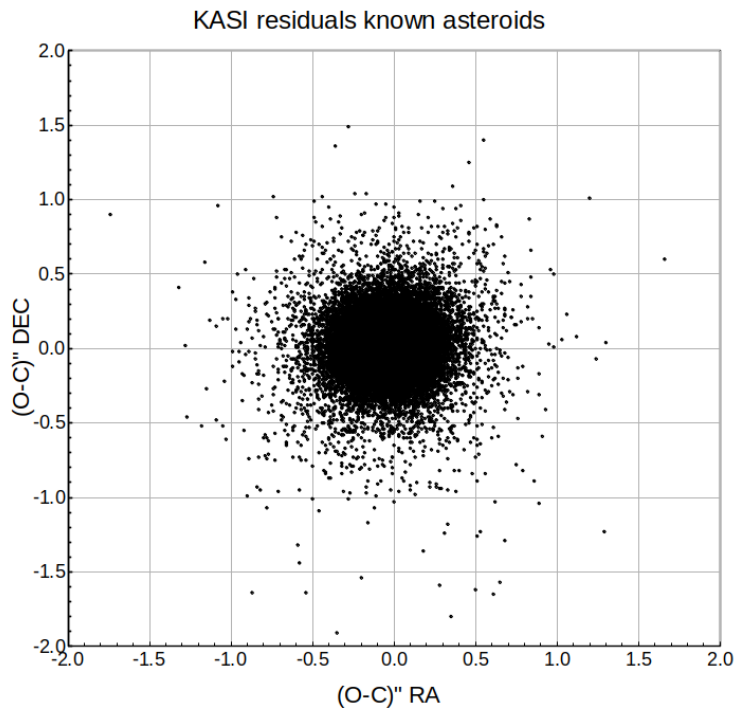


Figure 6: KASI NEA candidates detections (continued).



**Figure 6:** KASI NEA candidates detections (continued).



**Figure 7:** The residuals of known asteroids found in the entire KASI mini-survey.

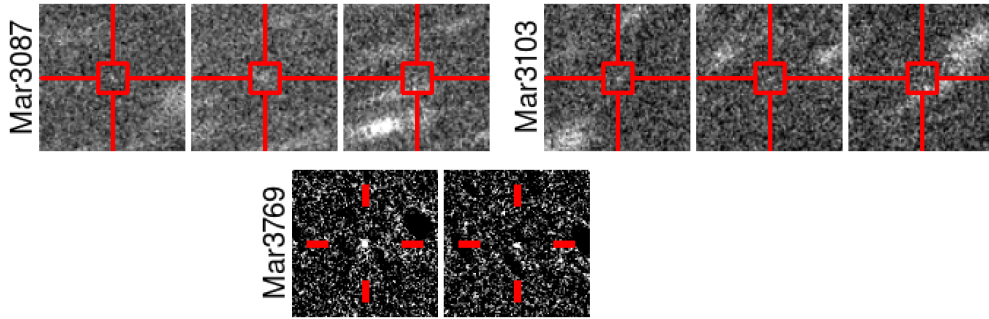


**Figure 8:** T80S NEA candidates detections.

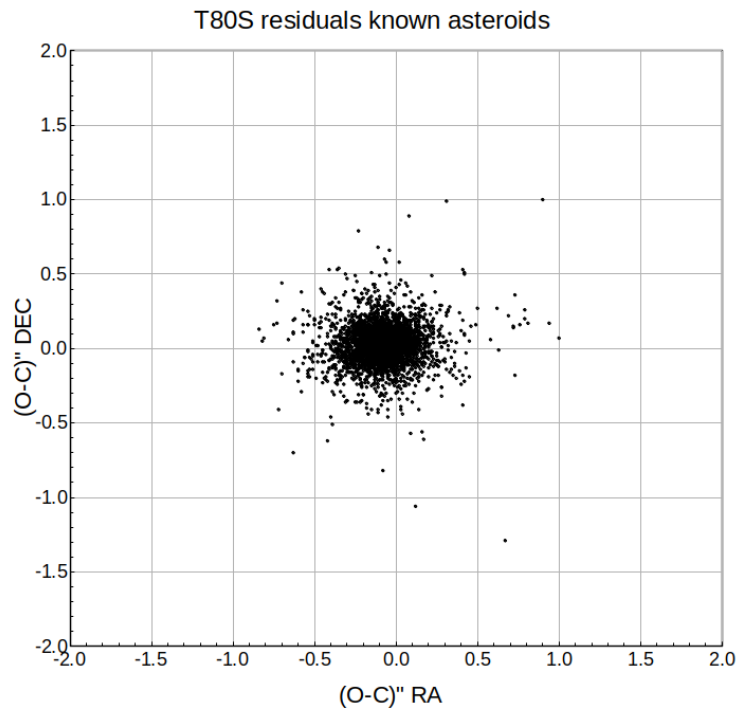


**Figure 9:** The residuals of known asteroids found in the entire T80S mini-survey.

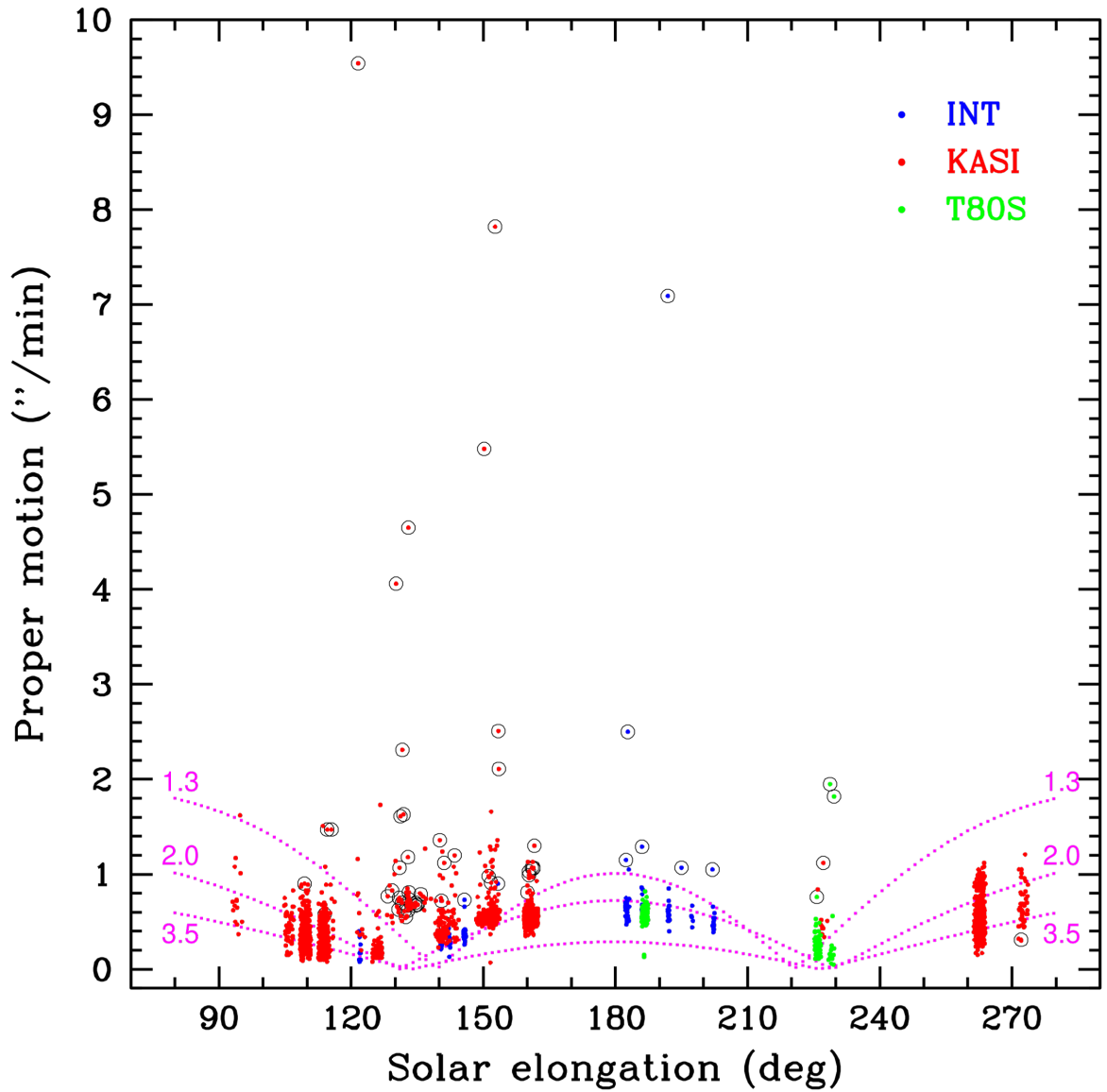


**Figure 10:** Solar elongation versus proper motion ( $\epsilon - \mu$ ) plot of the NEA candidate fields found in the 3 mini-surveys.

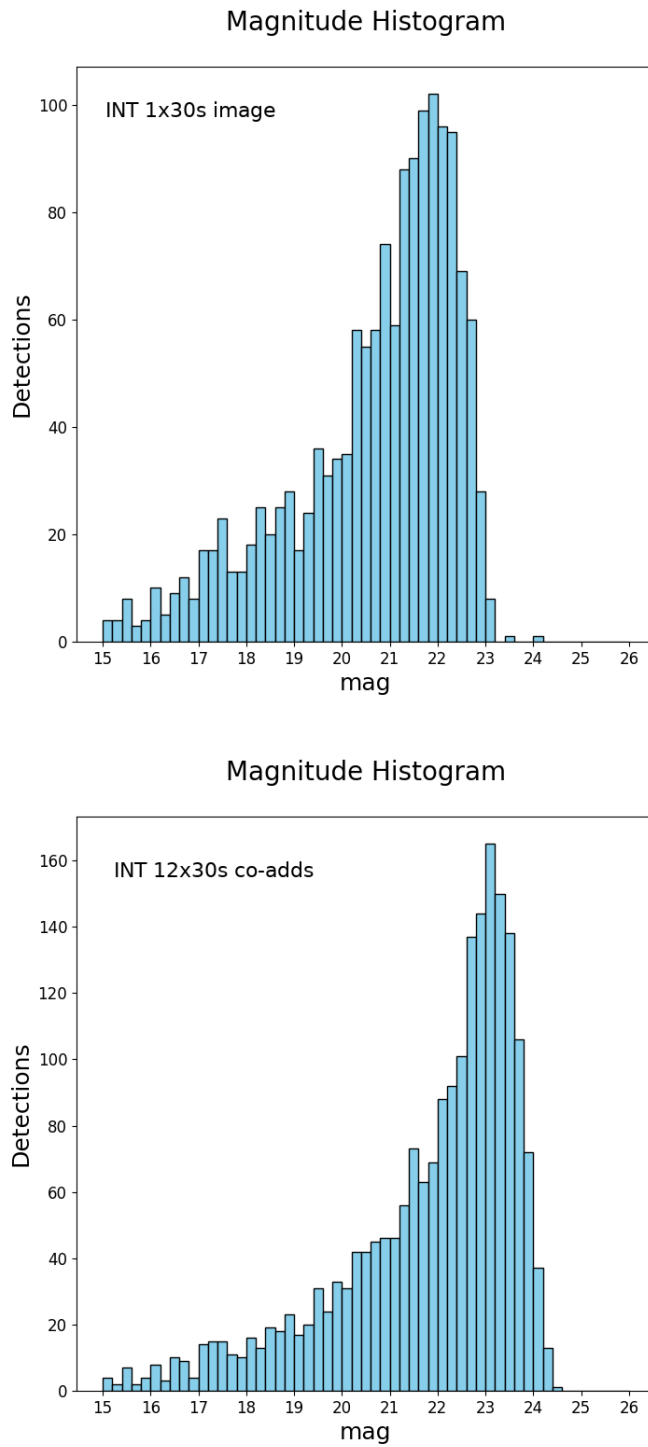


**Figure 11:** *MagLim* histogram showing INT depth of field ECL5 CCD4:  $r = 22.0$  for one 30 s image (upper side) versus  $r = 23.2$  for 12x30s co-adds (bottom side), showing an increase factor of 1.4x in the number of detections and 1.2 magnitudes.